Supplementary Information for:

Enzyme Amplified Array Sensing of Proteins in Solution and in Biofluids

Oscar R. Miranda,[1] Hung-Ting Chen,[1] Chang-Cheng You,[1] David E. Mortenson,[1] Xiao-Chao Yang,[3] Uwe H. F. Bunz,[2] and Vincent M. Rotello[1]*

[1]*Department of Chemistry, University of Massachusetts, 710 North Pleasant Street, Amherst, Massachusetts 01003, USA;* [2]*School of Chemistry and Biochemistry, Georgia Institute of Technology, 901 Atlantic Drive, Atlanta, Georgia 30332,USA;* [3]*College of Bioengineering and Microsystem Research Center, Chongqing University, Chongqing 400044, China.*

Experimental section

Binding of β-Gal to cationic AuNPs 1-6. Agarose (Type-IB, Sigma Aldrich) gel electrophoresis was performed using a FisherBiotech Electrophoresis System (mini-horizontal unit FB-SB-710). β-Gal (2 μM) was incubated with cationic AuNPs at different ratio in sodium phosphate buffer (5 mM, pH 7.4) for 15 minutes. 5 μL of 80% glycerol in deionized water (18 MΩ-cm) was added to 40 μL of above solutions and the samples were loaded onto the gel. A constant voltage (100 V) was applied to the system for 45 min to achieve adequate separation. The gels were then stained in a 0.5% Coomassie blue solution (40% volume methanol and 10% volume acetic acid in distilled water) for 1 h. Extensive destaining process was carried out with a 40% volume methanol and 10% volume acetic acid aqueous solution until the proteins were clearly visible.

Concentration of desalted human urinary proteins. The male human urine sample (Bioreclamation Inc.) was first adjusted to pH 3.5. Then, the pH-adjusted urine sample was applied on a pre-activated maxi spin column (Norgen Biotek Corporation, NBC). A buffer solution (P/N 21602) from NBC was

used to wash the column. At pH 3.5, the urinary proteins are able to bind to the resin in the column based on their charges; while the salts and other related species are removed with the eluent. The purified urine proteins were finally eluted with an elution buffer solution (P/N 21605) from NBC (Figures S26 and S27). The concentrated and salt-free human urine proteins were diluted at a concentration of 120 μg/mL (~1.5 μM) in 5 mM phosphate buffer. This complex matrix was used to prepare β-Gal solutions at 0.5 nM. Experiments using these samples need to be processed as soon as possible; delays of more than 2 h might cause unreliable results.

Protein sensing in presence of desalted human urinary proteins. β-galactosidase (β-Gal) and the fluorogenic substrate (4-methylumbelliferyl-β-D-galactopyranoside, MUG) were purchased from Sigma-Aldrich. In the two different studies, nanoparticle and β-Gal solutions were prepared i) in sodium phosphate buffer solution (5 mM, pH 7.4) and ii) 120 μg/mL human urinary proteins in 5 mM phosphate buffer. In the activity assay studies, β-Gal (0.5 nM) was incubated with various concentrations of **NP1**-**NP6** for 30 minutes and 1 mM of the fluorogenic substrate (MUG) was added. As a control experiment, the enzymatic activity of β-Gal was also monitored in the presence of neutral tetraethylene glycol functionalized nanoparticles. The β-Gal stock concentration was 275 nM, while the stock concentrations of **NP1**-**NP6** were prepared in the range of 100 nM and 50 nM. The inhibition studies were carried out at pre-determined times by adding 5 μL of MUG (42 mM in DMSO) and 5 μL of PB buffer into 200 μL β-Gal/AuNP solution. The enzymatic activity was followed by monitoring product formation every 22 s for 15 minutes at 455 nm using a microplate reader (EL808 Bio-Tek Instruments, Inc.). The samples were measured in triplicate. From the activity/inhibition studies, optimal concentrations of β-Gal/AuNP complexes were obtained.

Once the different inhibiting characteristics of the β-Gal/AuNP complexes were established, stoichiometric amounts of β-Gal and **NP1**-**NP6** were used to sense the protein targets in two different solutions. In the first solution the analyte targets were spiked in 5 mM phosphate buffer (pH 7.4) while the second was spiked in 5 mM phosphate buffer containing 120 μg/mL human urinary proteins. As a general protocol, each solution of the β-Gal/AuNP complex (200 μL) was placed into a well on the 96-well microplate. After incubation for 30 mins, 5 μL of an analyte protein solution (stock solution = 42 nM) was added to each well. After incubation for another 30 min, 5 μL of MUG (42 mM in DMSO) was added to the sample and the enzyme reaction activity was monitored for product formation every 22 s for 15 minutes at 455 nm using a microplate reader. This process was carried out for 9 proteins to generate six replicates for each, leading to a training data matrix of 6 nanoparticles × 9 proteins × 6 replicates that was subjected to a classical linear discriminant analysis (LDA) using SYSTAT (version 11.0). In the studies of unknown samples, sixty unknown protein solutions were randomly selected from nine proteins in the training set, and prepared at 42 nM concentration diluted from a stock solution with UV absorbance at 280 nm equal to 0.1. The sensing assay was conducted using the aforementioned procedure with 5 μL of unknown, affording a final protein concentration of 1 nM into the 96 wells microplate reader. Each unknown was performed twice against sensor array to obtain an average of a fluorescence response pattern. Afterward, the protein identity was detected by LDA analysis, with the system correctly determining a 92% of accuracy of the unknown samples over the span of the experiment. In the experimental setup, the solution preparation, data collection, and LDA analysis were operated by different persons to reduce bias and increase reproducibility of the unknown experiment.

Instrumentation. TEM samples were prepared by depositing 3 μL of a diluted aqueous solution of cationic AuNPs (5 μM) onto a 300 mesh carbon-coated copper grid. The samples were dried in air at room temperature. TEM images were obtained on a JEOL 100CX electron microscope operated at 100 keV and analyzed using Image J. More than 200 AuNPs were taken as target samples to calculate the average diameters and size distributions. ζ-Potential (ZP) and dynamic light scattering (DLS) results were used to characterize the charge and the hydrodynamic diameter of both nanoparticles and proteins. Cationic gold nanoparticles were dissolved in sodium phosphate buffer (5 mM, pH 7.4) to make solutions at 5 μM concentrations. The samples were filtered through a Millipore syringe-driven filter (0.22 μm) and injected into a folded capillary disposable cell. In the case of the proteins, the samples were filtered through a Millipore syringe-driven filter (0.22 μm) and injected into the disposable cell. Both ZP and DLS were measured on a MALVERN Zetasizer Nano ZS instrument. Each sample was scanned six times and an average value was reported.

Synthesis of AuNPs 1-6. Pentanethiol-coated AuNPs with core diameter ~2 nm were synthesized using the Brust-Schiffrin two-phase synthesis method.[1] Murray place-exchange method[2] was used to obtain the quaternary ammonium functionalized AuNPs **1-6** (see Schemes I, II, and III for synthesis and Figures S1-S25 for characterization).[3] The cationic AuNPs were very stable in aqueous solution.

Target proteins. α-Amylase (α-Amy, from *Bacillus licheniformis*), bovine serum albumin (BSA, from *Bovine serum*), cytochrome *c* (CytC, from equine heart), ferritin (Fer, from equine spleen), human

[1] a) Kanaras, A. G.; Kamounah, F. S.; Schaumburg, K.; Kiely, C. J.; Brust, M. *Chem. Commun.* **2002**, 2294. b) Brust, M.; Walker, M.; Bethell, D.; Schiffrin, D. J.; Whyman, R. *J. Chem. Soc. Chem. Commun.* **1994**, 801.

[2] Templeton, A. C.; Wuelfing, M. P.; Murray, R. W. *Acc. Chem. Res.* **2000**, *33*, 27.

[3] a) You, C. C.; Miranda, O. R.; Gider, B.; Ghosh, P. S.; Kim, I. B.; Erdogan, B.; Krovi, S. A.; Bunz, U. H. F.; Rotello, V. M. *Nat. Nanotech.* **2007**, *2*, 318. b) Zhu, Z. J.; Ghosh, P. S.; Miranda, O. R.; Vachet, R. W.; Rotello, V. M. *J. Am. Chem. Soc.* **2008**, 130, 14139. c) Phillips, R. L.; Miranda, O. R.; Mortenson, D. E.; Subramani, C.; Rotello, V. M.; Bunz, U. H. F. *Soft Matter* **2009**, 5, 607. d) De, M.; Rana, S.; Akpinar, H.; Miranda, O. R.; Arvizo, R.; Bunz, U. H. F.; Rotello, V. M. *Nat. Chem.* **2009**, 1, 461.

serum albumin (HAS, from *human serum*), lipase (Lip, from *candida rugosa*, type VII), lysozyme (Lys, from chicken egg white), myoglobin (Myo, from equine heart), and alkaline phosphatase (PhosB, from bovine intestinal mucosa) were purchased from Sigma-Aldrich and used as received. The protein concentrations were standaridized by the absorbance at 280 nm in 5 mM phosphate buffer at pH 7.4 using a Hewlett Packard 8452A Diode Array Spectophotometer.

Scheme I. Synthesis of Ligands **L1**, **L2**, **L3**, **L4, L5** and **L6**.

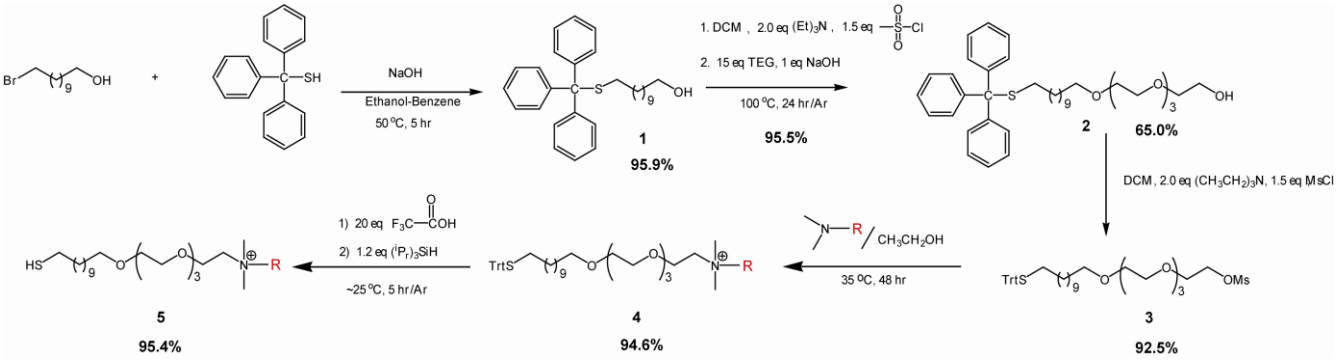

General procedure:

Compound 1: Triphenylmethanethiol (7.92 g, 28.66 mmol) was dissolved in a solution of ethanol/benzene (1:1, 50 mL) and NaOH (1.43 g, 35.82 mmol) in 15 mL of H_2O was added. Then 11-bromo-1-undecanol (6 g, 23.88 mmol) was also dissolved in a solution of ethanol/benzene (1:1, 50 mL) and added to the triphenylmethanethiol mixture. The new reaction mixture was stirred overnight at room temperature. Once the reaction was completed (checked by TLC) all the mixture was poured into a saturated solution of $NaHCO_3$ and washed three times. The organic layer was separated and added into another solution saturated of NaCl and also washed for three times. Afterward the organic layer was separated, dried (Na_2SO_4), and concentrated using a rotavapor. The crude product was purified by column chromatography over silica gel using hexane/ethyl acetate (9:1, 4:1 and 1:1, v/v) as an eluent. The solvent was removed in vacuum to obtain compound **1** as a colorless oil (Yield 10.23 g, >95.9 %, see NMR Figure S1).

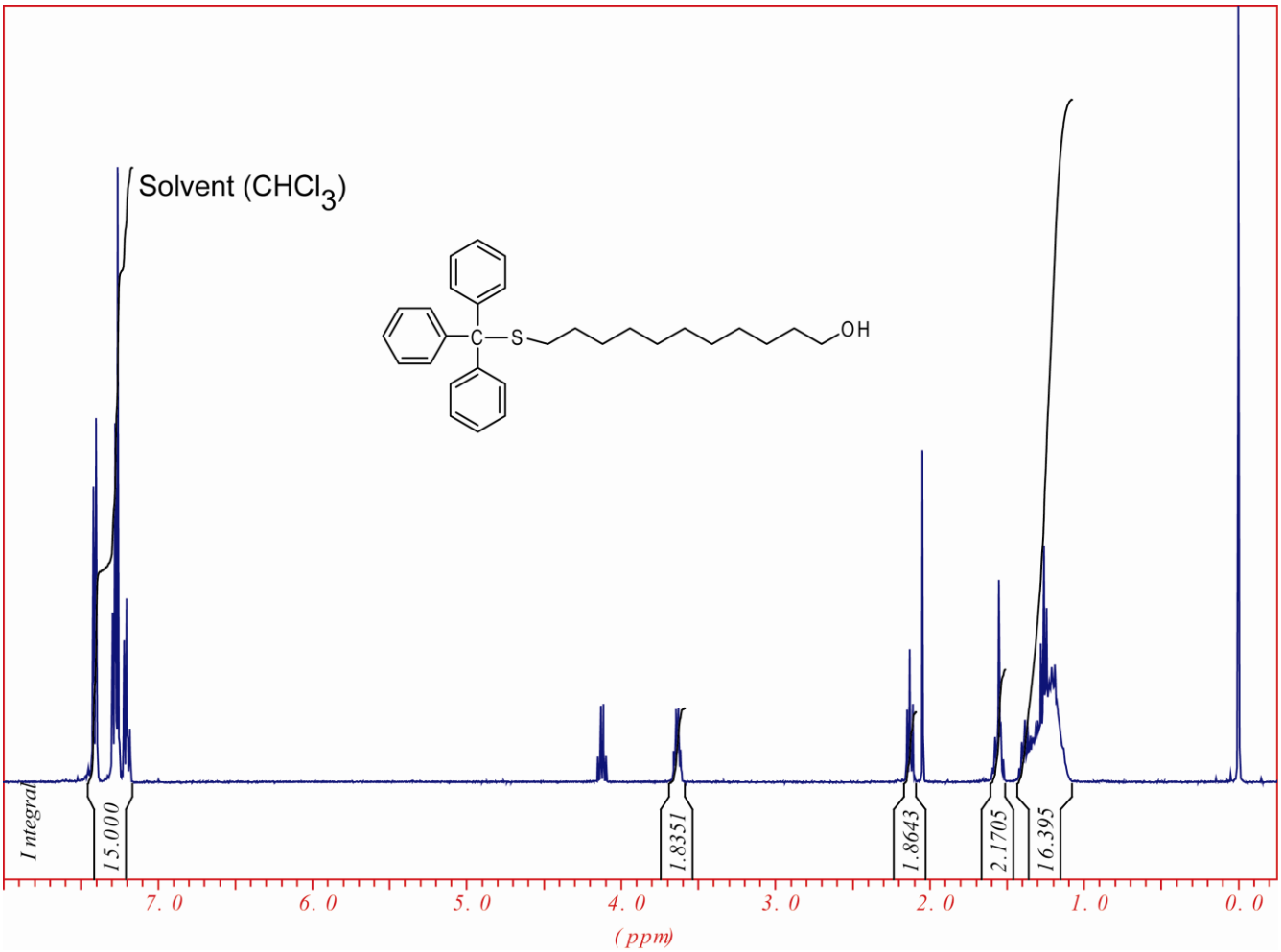

Figure S1. 400 MHz ^{1}H NMR spectra of **compound 1** in chloroform-D (D, 99.8%).

Compound 2: To a solution of compound **1** (9 g, 20.15 mmol) in dry dichloromethane (DCM) at 4 °C, triethylamine (4.08 g, 40.3 mmol) was added. Methylsulfonyl chloride (3.46 g, 30.2 mmol) was injected drop by drop to the solution maintaining the temperature less that 5 °C. After 30 minutes the reaction mixture was warmed up to room temperature and stirred for another 30 minutes. Once the reaction was completed (according to TLC), the DCM was evaporated. The viscous compound was again diluted with DCM and poured into 0.1 M solution of HCl, and treated twice. Organic layer was poured into a saturated solution of $NaHCO_3$ and washed three times. The organic layer was separated and added into another solution saturated of NaCl and also treated three times. Afterward organic layer was separated, dried (Na_2SO_4) and concentrated at reduced pressure. The crude product was purified by column chromatography over silica gel using hexane/ethyl acetate (1:1, v/v) as an eluent. Solvent was removed in vacuum to afford compound **2** as colorless oil (Yield 10.1 g, >95.5 %). The NMR showed an additional peak on the spectra of compound **1** around 2.95 ppm confirming the synthesis of 11-(tritylthio)undecyl methanesulfonate (see Figure S2). To synthesize 1,1,1-triphenyl-14,17,20,23-tetraoxa-2-thiapentacosan-25-ol, NaOH (0.8 g, 20 mmol) in 1 ml of H_2O was added to 58.26 mL of tetraethyleneglycol (TEG: 52.3 g, 300 mmol) and stirred for 1 h at 90 °C. To this reaction mixture, 11-(tritylthio)undecyl methanesulfonate (10 g, was added (by dissolving in TEG) and stirred for 24 h. The reaction mixture once completed (according to TLC) was extracted by washing with a solution of

hexane/ethyl acetate (4:1, v/v) six times (checked by TLC). Afterward, the organic layer was separated and concentrated at reduced pressure. The crude product was purified by column chromatography over silica gel (flash running) using hexane/ethyl acetate (1:1 and 0:1, v/v) as an eluent. The solvent was removed in vacuum to obtain compound **2** as a colorless oil (Yield 7.83 g, >65.0 %, see NMR Figure S3).

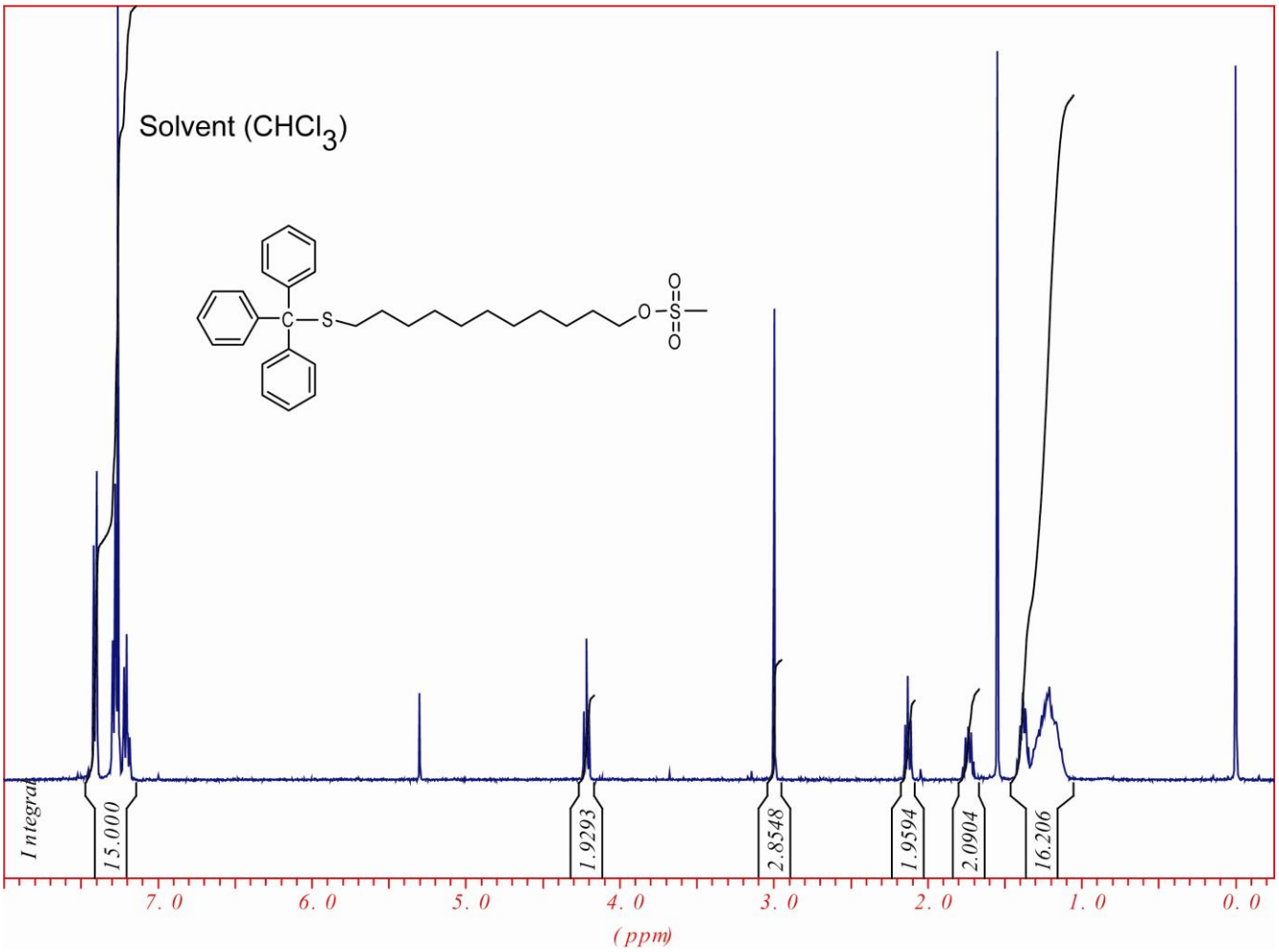

Figure S2. 400 MHz ^{1}H NMR spectra of **11-(tritylthio)undecyl methanesulfonate** in chloroform-D (D, 99.8%).

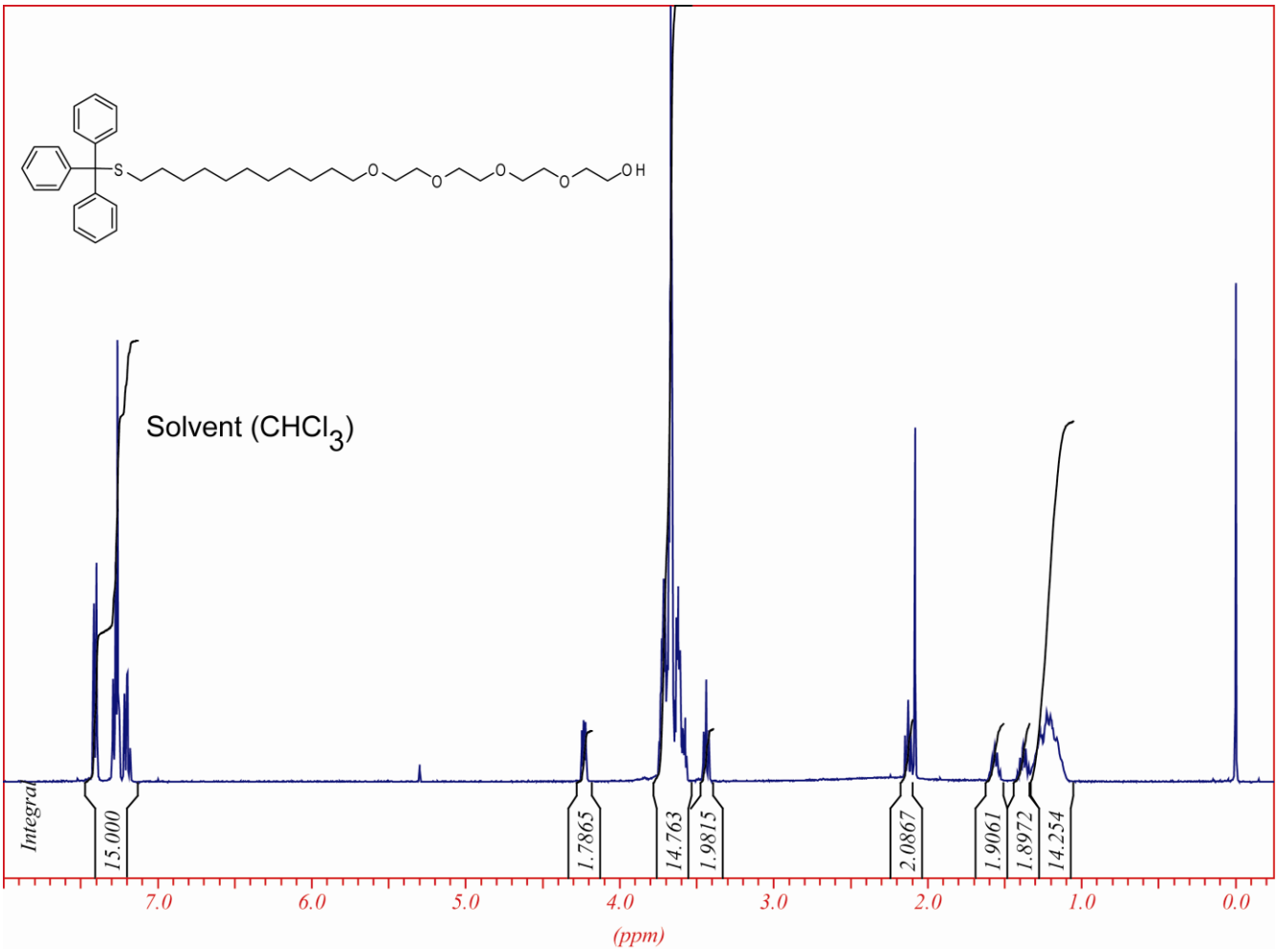

Figure S3. 400 MHz ^{1}H NMR spectra of **compound 2** in chloroform-D (D, 99.8%).

Compound 3: Compound **2** (7 g, 11.24 mmol) was dissolved in dry dichloromethane (DCM) at 4 °C, and was followed by the addition of triethylamine (3.41 g, 33.72 mmol). Methylsulfonyl chloride (2.44 g, 16.86 mmol) was injected drop by drop to the reaction mixture maintaining the temperature less that 5 °C. After 30 minutes the reaction mixture was warmed up to room temperature and stirred for another 30 minutes. When the reaction was finally completed (according to TLC), the DCM solvent was evaporated. The viscous compound was again diluted with DCM and was poured into 0.1 M solution of HCl, and washed twice. The organic layer was poured into a saturate solution of $NaHCO_3$ and treated three times. Organic layer was separated and added into another solution saturated of NaCl and also treated for three times. Afterward, the organic layer was separated, dried (Na_2SO_4) and concentrated at reduced pressure. The crude product was purified by column chromatography over silica gel (flash running) using hexane/ethyl acetate (1:1, 1:4 and 0:1 v/v) as an eluent. Solvent was removed in vacuum to afford compound **3** as a colorless oil (Yield 7.31 g, >92.5 %). The NMR results showed an additional peak on the spectra of compound **1** around ~2.75 ppm confirming the synthesis of 1,1,1-triphenyl-14,17,20,23-tetraoxa-2-thiapentacosan-25-yl methanesulphonate (see Figure S4).

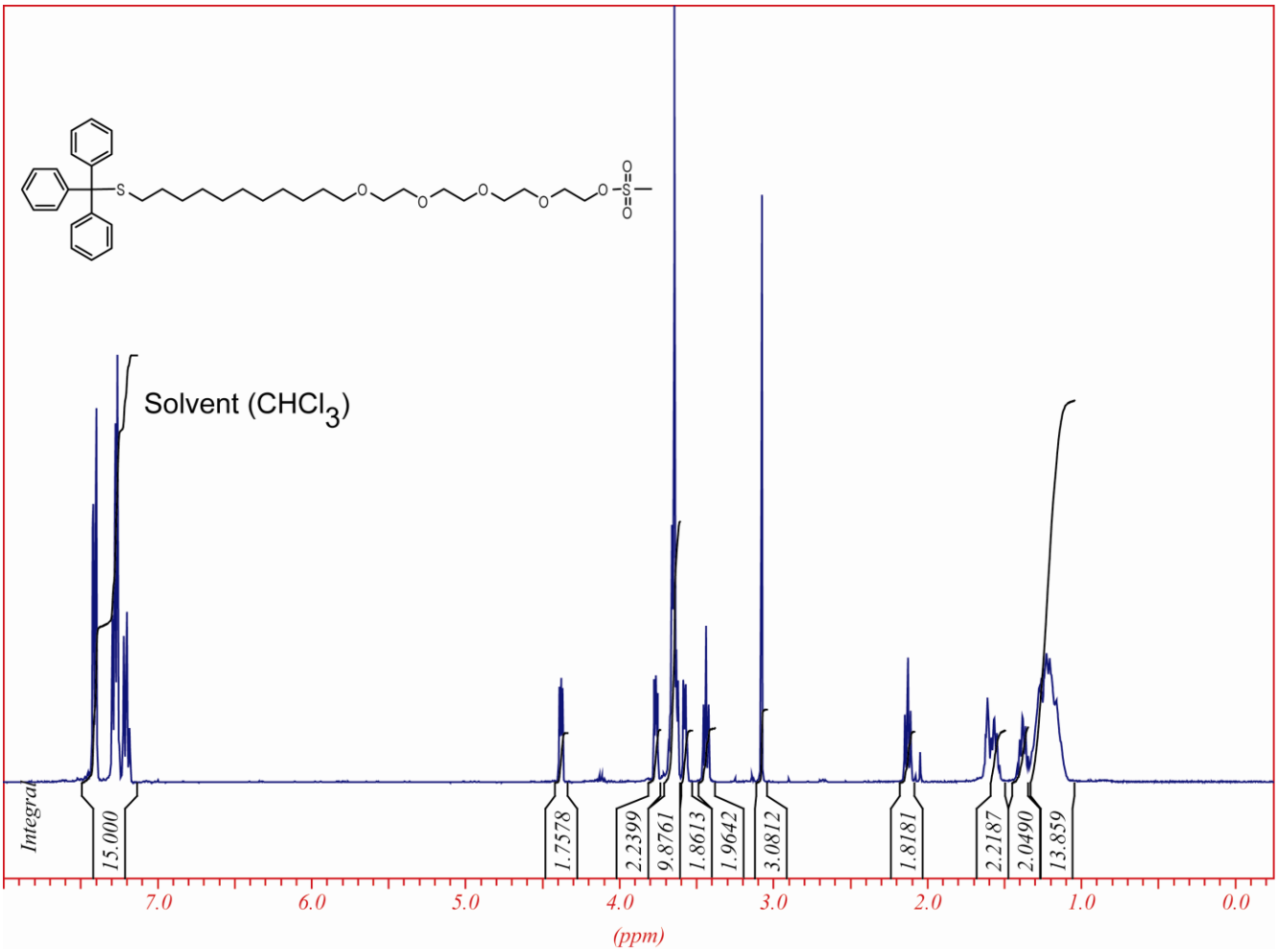

Figure S4. 400 MHz ^{1}H NMR spectra of **compound 2** in chloroform-D (D, 99.8%).

Compound 4 (Trt L): Compound **3** (1 g, 1.43 mmol) was added to an available library of dimethylamine solutions (28.53 mmol) containing 5% of ethanol. The reaction mixtures were stirred at ~35 ^{o}C for 48 h. Crude product was checked by TLC and ethanol was eliminated at reduced pressure. The light yellow residue was purified by hexane with support of both heat and sonication and further dried in a high vacuum system. The product formation (**4**) was quantitative and their structure was confirmed by NMR. The yield was >94.6 %.

^{1}H NMR of compound 4 (Trt L)

Compound Trt L1: ^{1}H NMR (400MHz, $CDCl_3$, TMS): δ 7.43-7.38 (m, 4H, H_{Ar}), 7.31-7.24 (m, 9H, H_{Ar}), 7.23-7.17 (m, 2H, H_{Ar}), 3.98 (br, 2H, -OC$\underline{H}_2$-(CH_2N)-), 3.67-3.58 (m, 14H, -CH_2O- + -CH_2N-), 3.55 (t, 2H, -CH_2O-), 3.50-3.41 (m, 2H,-NCH_2-), 3.27 (s, 6H, -(CH_3)$_2$N-), 2.75 (s, 3H, $CH_3SO^-_3$-), 2.21 (t, 2H, -SCH_2-), 1.74-1.50 (m, 6H, -(NCH_2)C$\underline{H}_2$-) + (SCH_2)C$\underline{H}_2$ + -C$\underline{H}_2$(CH_2O)-), 1.42-1.11 (m, 20H, -(NCH_2CH_2-)C$\underline{H}_2$-) + -CH_2-), 0.89 (t, 3H, - CH_3-).

Compound Trt L2: ^{1}H NMR (400MHz, $CDCl_3$, TMS): δ 7.44-7.37 (m, 4H, H_{Ar}), 7.32-7.23 (m, 9H, H_{Ar}), 7.22-7.16 (m, 2H, H_{Ar}), 3.99 (br, 2H, -OC$\underline{H}_2$-(CH_2N)-), 3.67-3.58 (m, 12H, -CH_2O-), 3.57-3.54 (m, 1H, H_{Cyclo}), 3.51-3.39 (m, 4H, -CH_2O- +-CH_2N-), 3.19 (s, 6H, -(CH_3)$_2$N-), 2.75 (s, 3H, $CH_3SO^-_3$-),

2.12 (t, 2H, -SCH_2-), 1.77-1.65 (m, 2H, H_{Cyclo}), 1.59-1.50 (m, 2H, H_{Cyclo}), 1.48-1.07 (m, 22H, H_{Cyclo}, -$(SCH_2)C\underline{H_2}$ + -$(SCH_2)CH_2C\underline{H_2}$ + -$C\underline{H_2}(CH_2O)$- + -$C\underline{H_2}(CH_2CH_2O)$- + -CH2-).

Compound Trit L3: ^{1}H NMR (400MHz, $CDCl_3$, TMS): δ 7.66-7.59 (m, 2H, H_{Ar}), 7.50-7.36 (m, 7H, H_{Ar}), 7.32-7.23 (m, 9H, H_{Ar}), 7.22-7.16 (m, 2H, H_{Ar}), 4.80 (br, 2H,-NCH_2-Ar), 3.84 (br, 2H, -$OC\underline{H_2}$-(CH_2N)-), 3.73-3.55 (m, 14H, -CH_2O- + -CH_2N-), 3.54-3.49 (m, 2H, -CH_2O-), 3.23 (s, 6H, -$(CH_3)_2N$-), 2.79 (s, 3H, $CH_3SO^-_3$-), 2.12 (t, 2H, -SCH_2-), 1.57-1.48 (m, 2H, -$(SCH_2)C\underline{H_2}$), 1.43-1.32 (m, 2H, -$C\underline{H_2}(CH_2O)$-), 1.31-1.07 (m, 12H, -CH_2-).

Compound Trit L4: ^{1}H NMR (400MHz, $CDCl_3$, TMS): δ 7.43-7.37 (m, 4H, H_{Ar}), 7.31-7.24 (m, 9H, H_{Ar}), 7.23-7.17 (m, 2H, H_{Ar}), 3.95 (br, 2H, -$OC\underline{H_2}$-(CH_2N)-), 3.77 (b, 1H, OH), 3.76-3.53 (m, 16H, -CH_2O- + -CH_2N- + -$C\underline{H_2}$-OH), 3.51-3.44 (m, 2H,-NCH_2-), 3.42 (m, 2H, -CH_2O-), 3.24 (s, 6H, -$(CH_3)_2N$-), 2.74 (s, 3H, $CH_3SO^-_3$-), 2.13 (t, 2H, -SCH_2-), 2.09-1.99 (m, 2H, -$(NCH_2)C\underline{H_2}$-), 1.59-1.51 (m, 2H, -$(SCH_2)C\underline{H_2}$), 1.42-1.33 (m, 2H, -$C\underline{H_2}(CH_2O)$-), 1.33-1.10 (m, 14H, -CH_2-).

Compound Trit L5: ^{1}H NMR (400MHz, $CDCl_3$, TMS): δ 7.65-7.57 (m, 2H, H_{Ar}), 7.53-7.35 (m, 7H, H_{Ar}), 7.31-7.23 (m, 9H, H_{Ar}), 7.21-7.15 (m, 2H, H_{Ar}), 3.97 (br, 2H, -$OC\underline{H_2}$-(CH_2N)-), 3.65-3.56 (m, 13H, -CH_2O- + H_{Cyclo}), 3.57-3.53 (m, 1H, H_{Cyclo}), 3.50-3.39 (m, 4H, -CH_2O- +-CH_2N-), 3.17 (s, 6H, -$(CH_3)_2N$-), 2.75 (s, 3H, $CH_3SO^-_3$-), 2.13 (t, 2H, -SCH_2-), 1.77-1.64 (m, 2H, H_{Cyclo}), 1.59-1.49 (m, 2H, H_{Cyclo}), 1.47-1.05 (m, 22H, H_{Cyclo}, -$(SCH_2)C\underline{H_2}$ + -$(SCH_2)CH_2C\underline{H_2}$ + -$C\underline{H_2}(CH_2O)$- + -$C\underline{H_2}(CH_2CH_2O)$- + -CH2-).

Compound Trit L6: ^{1}H NMR (400MHz, $CDCl_3$, TMS): δ 7.43-7.38 (m, 4H, H_{Ar}), 7.36-7.31 (m, 7H, H_{Ar}), 7.30-7.24 (m, 12H, H_{Ar}), 7.23-7.17 (m, 2H, H_{Ar}), 5.39 (s, 1H, CH-Ar-), 3.99-3.93 (m and br, 2H, -CH_2OCAr-), 3.92-3.87 (m and br, 2H, -$OC\underline{H_2}$-(CH_2N)-), 3.65-3.55 (m, 14H, -CH_2O- + -CH_2N-), 3.54-3.51 (m, 2H, -CH_2O-), 3.49-3.44 (m, 2H, -$NC\underline{H_2}(CH_2OCAr$-), 3.37 (s, 6H, -$(CH_3)_2N$-), 2.74 (s, 3H, -$CH_3SO^-_3$-), 2.13 (q, 2H, -$CH_2S$-), 1.59-1.50 (m, 2H, -$(SCH_2)C\underline{H_2}$), 1.41-1.34 (m, 2H, -$C\underline{H_2}(CH_2O)$-), 1.33-1.10 (m, 14H, -$CH_2$-).

Compound 5: Compound **4** was dissolved in dry dichloromethane (DCM) and an excess of trifluoroacetic acid (TFA, ~ 20 equivalents) was added. The color of the solution was turned to yellow immediately. Subsequently, triisopropylsilane (TIPS, ~ 1.2 equivalents) was added to the reaction mixture. The reaction mixture was stirred for ~5 h under Ar_2 at room temperature. The solvent and most TFA and TIPS were distilled off under reduced pressure. The pale yellow residue was purified by hexane combining both heat and sonication and further dried in a high vacuum system. The product (**L**) formation was quantitative and their structure was confirmed by NMR showing a shift of the counter ion peak on the spectra to more down field ~2.98 ppm. The yields were >95.4%.

^{1}H NMR and **^{13}C** of **compound 5 (Figures S5-S16)**

Compound L1: ^{1}H NMR (400MHz, $CDCl_3$, TMS): δ 3.95 (br, 2H, -$OC\underline{H_2}$-(CH_2N)-), 3.68-3.56 (m, 14H, -CH_2O- + -CH_2N-), 3.46 (t, 2H, -CH_2O-), 3.40-3.33 (m, 2H,-NCH_2-), 3.19 (s, 6H, -$(CH_3)_2N$-), 2.87 (s, 3H, $CH_3SO^-_3$-), 2.52 (q, 2H, -CH_2S-), 1.76-1.53 (m, 6H, -$(NCH_2)C\underline{H_2}$-) + $(SCH_2)C\underline{H_2}$ + -$C\underline{H_2}(CH_2O)$-), 1.41-1.22 (m, 21H, -SH + -$(NCH_2CH_2$-)$C\underline{H_2}$-) + -CH_2-), 0.89 (t, 3H, -CH_3-). ^{13}C NMR(400 MHz, $CDCl_3$) δ(ppm): 71.59, 70.54, 70.51, 70.44, 70.33, 70.15, 70.00, 66.42, 64.82, 63.50, 51.90, 34.07, 31.18, 29.59, 29.54, 29.52, 29.49, 29.09, 28.39, 26.07, 25.84, 24.68, 22.71, 22.37, 13.85.

Compound L2: ^{1}H NMR (400MHz, $CDCl_3$, TMS): (3.97 (br, 2H, -OC<u>H</u>$_2$-(CH_2N)-), 3.69-3.55 (m, 14H, -CH_2O- + -CH_2N-), 3.54-3.48 (m, 1H, HCyclo), 3.44 (t, 2H, -CH_2O-), 3.13 (s, 6H, -(CH_3)$_2$N-), 2.86 (s, 3H, $CH_3SO^-_3$-), 2.52 (q, 2H, -CH_2S-), 2.25 (d, 2H, HCyclo), 1.99 (d, 2H, HCyclo), 1.73 (d, 2H, HCyclo), 1.78-1.52 (m, 4H, -(SCH_2)C<u>H</u>$_2$ + -C<u>H</u>$_2$(CH_2O)-), 1.51-1.12 (m, 19H, SH + -CH_2- + HCyclo). ^{13}C NMR(400 MHz, $CDCl_3$) δ(ppm): 73.76, 71,02, 69.85, 69.82, 69.69, 69.61, 69.37, 64.16, 61.42, 48.29, 38.89, 33.46, 28.98, 28.92, 28.87, 28.76, 28.48, 28.07, 27.94, 27.78, 25.75, 25.43, 24.68, 24.11.

Compound L3: ^{1}H NMR (400MHz, $CDCl_3$, TMS): δ 7.56-7.45 (m, 5H, H_{Ar}), 4.60 (s and br, 2H,-NC<u>H</u>$_2$-Ar), 4.03 (br, 2H, -OC<u>H</u>$_2$-(CH_2N)-), 3.75-3.50 (m, 14H, -CH_2O- + -CH_2N-), 3.48-3.41 (m, 2H, -CH_2O-), 3.14 (s, 6H, -(CH_3)$_2$N-), 2.91 (s, 3H, $CH_3SO^-_3$-), 2.52 (q, 2H, -CH_2S-), 1.72-1.46 (m, 4H, -(SCH_2)C<u>H</u>$_2$ + -C<u>H</u>$_2$(CH_2O)-), 1.44-1.15 (m, 15H, -SH + -CH_2-). ^{13}C NMR(400 MHz, $CDCl_3$) δ(ppm): 132.85, 130.97, 129.27, 126.51, 116.08, 113.24, 71.52, 70.10, 70.05, 69.97, 69.90, 69.54, 64.53, 63.42, 50.68, 39.37, 33.84, 29.33, 29.28, 29.19, 29.12, 29.01, 28.86, 28.17, 25.69, 24.46.

Compound L4: ^{1}H NMR (400MHz, $CDCl_3$, TMS): δ 4.55-4.46 (m, 2H,-C<u>H</u>$_2$-OH), 3.99 (br, 2H, -OC<u>H</u>$_2$-(CH_2N)-), 3.85 (br, 1H, -OH), 3.79-3.52 (m, 16H, -CH_2O- + -CH_2N- + -NCH_2-), 3.47 (t, 2H, -CH_2O-), 3.25 (s, 6H, -(CH_3)$_2$N-), 2.87 (s, 3H, $CH_3SO^-_3$-), 2.52 (q, 2H, -CH_2S-), 2.35-2.26 (m, 2H, -(NCH_2)C<u>H</u>$_2$-), 1.70-1.49 (m, 4H, + (SCH_2)C<u>H</u>$_2$ + -C<u>H</u>$_2$(CH_2O)-), 1.42-1.19 (m, 15H, -SH + -CH_2-). ^{13}C NMR(400 MHz, $CDCl_3$) δ(ppm): 71.12, 69.70, 69.66, 69.62, 69.58, 69.48, 69.15, 63.92, 63.15, 62.11, 51.75, 38.87, 33.46, 28.94, 28.89, 28.80, 28.73, 28.64, 28.48, 28.34, 27.79, 25.29, 24.08, 21.45.

Compound L5: ^{1}H NMR (400MHz, $CDCl_3$, TMS): δ 7.4-7.19 (m, 5H, H_{Ar}), 3.95 (br, 2H, -OC<u>H</u>$_2$-(CH_2N)-), 3.79-3.52 (m, 15H, -CH_2O- + -CH_2N- + 1H, H_{Cyclo}), 3.45 (t, 2H, -CH_2O-), 2.81 (m and br, 6H, -(CH_3)$_2$N-), 2.87 (s, 3H, $CH_3SO^-_3$-), 2.70 (q, 2H, -CH_2S-), 2.59-2.41 (m and br, 1H, H_{Cyclo}), 2.39-2.20 (m, 2H, H_{Cyclo}), 2.19-2.06 (m, 2H, H_{Cyclo}), 1.96-1.84 (m, 4H, H_{Cyclo}), 1.72-1.53 (m, 4H, -(SCH_2)C<u>H</u>$_2$ + -C<u>H</u>$_2$(CH_2O)-), 1.42-1.1.19 (m, 15H, -SH + -CH_2-). ^{13}C NMR(400 MHz, $CDCl_3$) δ(ppm): 128.76, 128.73, 127.16, 127.09, 126.72, 126.39, 71.65, 70.50, 70.41, 70.37, 70.31, 70.27, 70.00, 64.97, 62.34, 62.07, 49.15, 48.81, 40.86, 34.16, 32.49, 32.13, 29.66, 29.58, 29.30, 28.68, 28.61, 27.77, 26.79, 26.34, 26.10, 24.03.21.77.

Compound L6: ^{1}H NMR (400MHz, $CDCl_3$, TMS): δ 7.42-7.27 (m, 10H, H_{Ar}), 5.13 (s, 1H, H_{Ar}), 4.12 (br, 2H, -CH_2OCAr-), 3.96 (br, 2H, -OC<u>H</u>$_2$-(CH_2N)-), 3.75-3.51 (m, 16H, -CH_2O- + -CH_2N- + -CH_2O-), 3.50-3.44 (m, 2H, -NC<u>H</u>$_2$(CH_2OCAr-), 3.28 (s, 6H, -(CH_3)$_2$N-), 2.95 (s, 3H, $CH_3SO^-_3$-), 2.38 (t, 2H, -CH_2S-), 1.60-1.48 (m, 4H, -(SCH_2)C<u>H</u>$_2$ + -C<u>H</u>$_2$(CH_2O)-), 1.34-1.16 (m, 15H, -SH + -CH_2-). -). ^{13}C NMR(400 MHz, $CDCl_3$) δ(ppm): 141.71, 128.61, 128.67, 127.18, 116.95, 114.10, 71.61, 70.51, 70.45, 70.32, 70.19, 69.97, 67.14, 64.80, 59.91, 56.26, 55.98, 54.25, 53.09, 50.46, 43.72, 39.47, 32.43, 29.63, 29.57, 29.52, 29.24, 29.09, 28.92, 26.08.

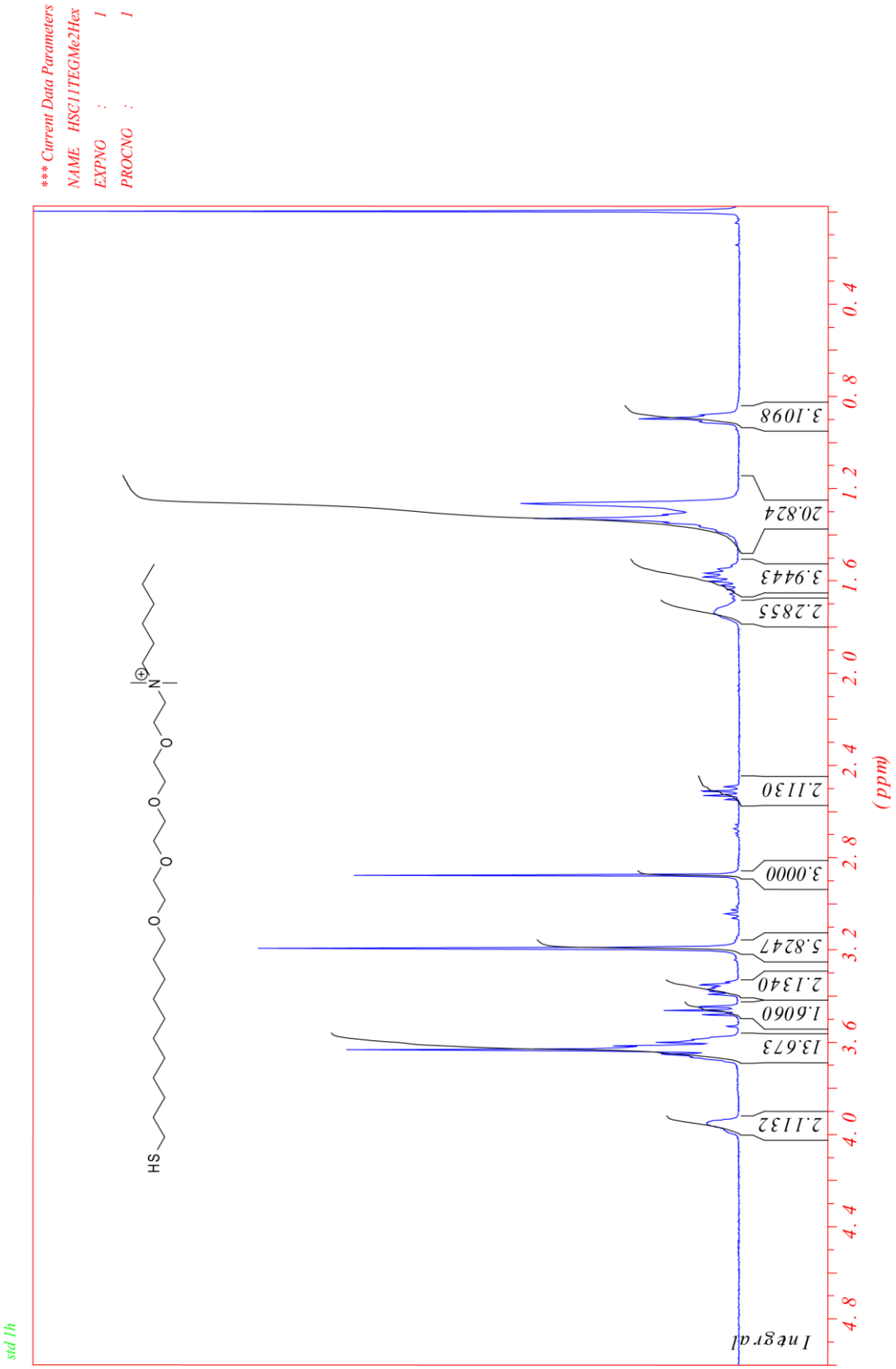

Figure S5. 400 MHz ^{1}H NMR spectra of **compound L1** in chloroform-D (D, 99.8%).

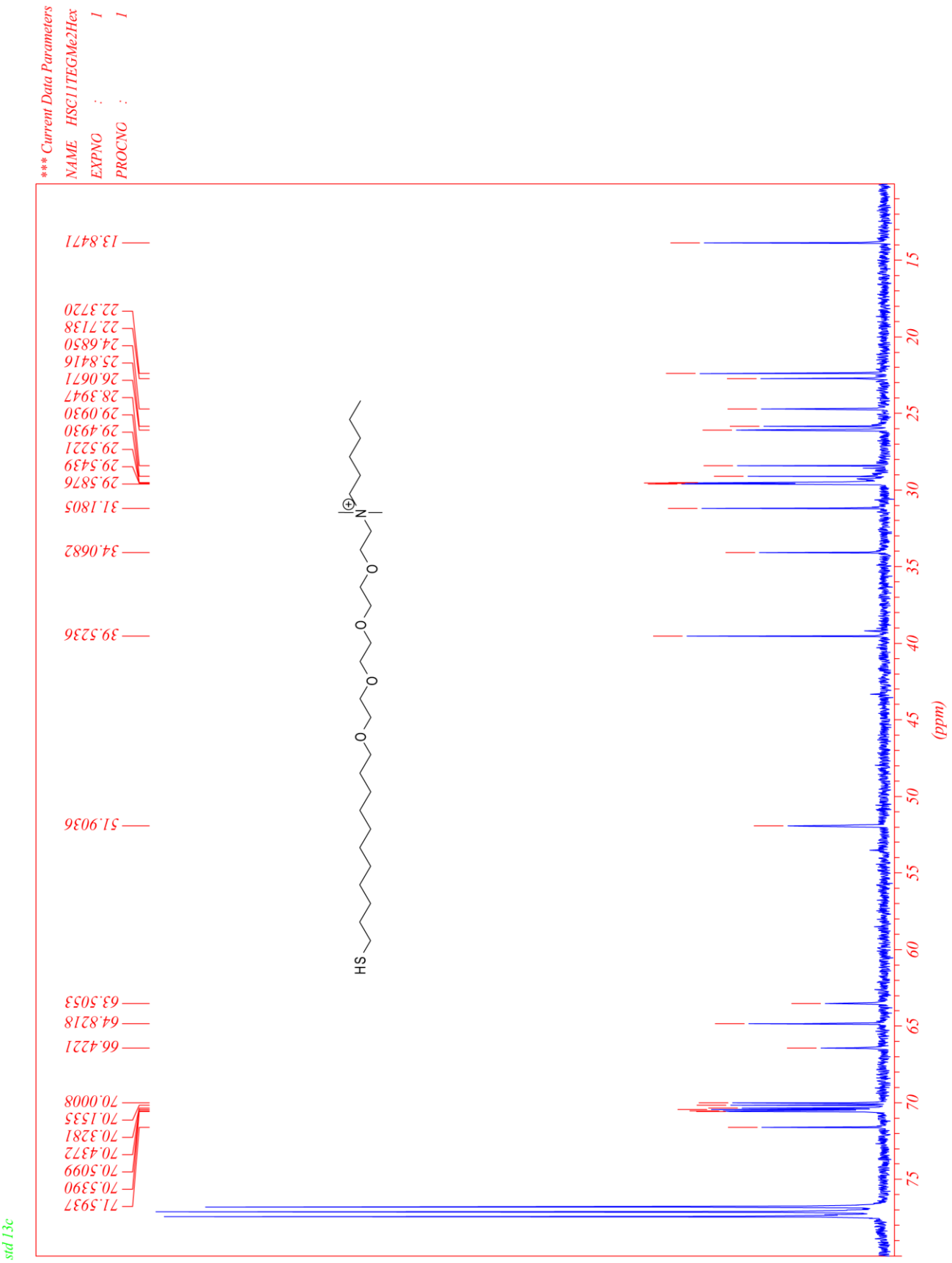

Figure S6. 400 MHz ^{13}C NMR spectra of **compound L1** in chloroform-D (D, 99.8%).

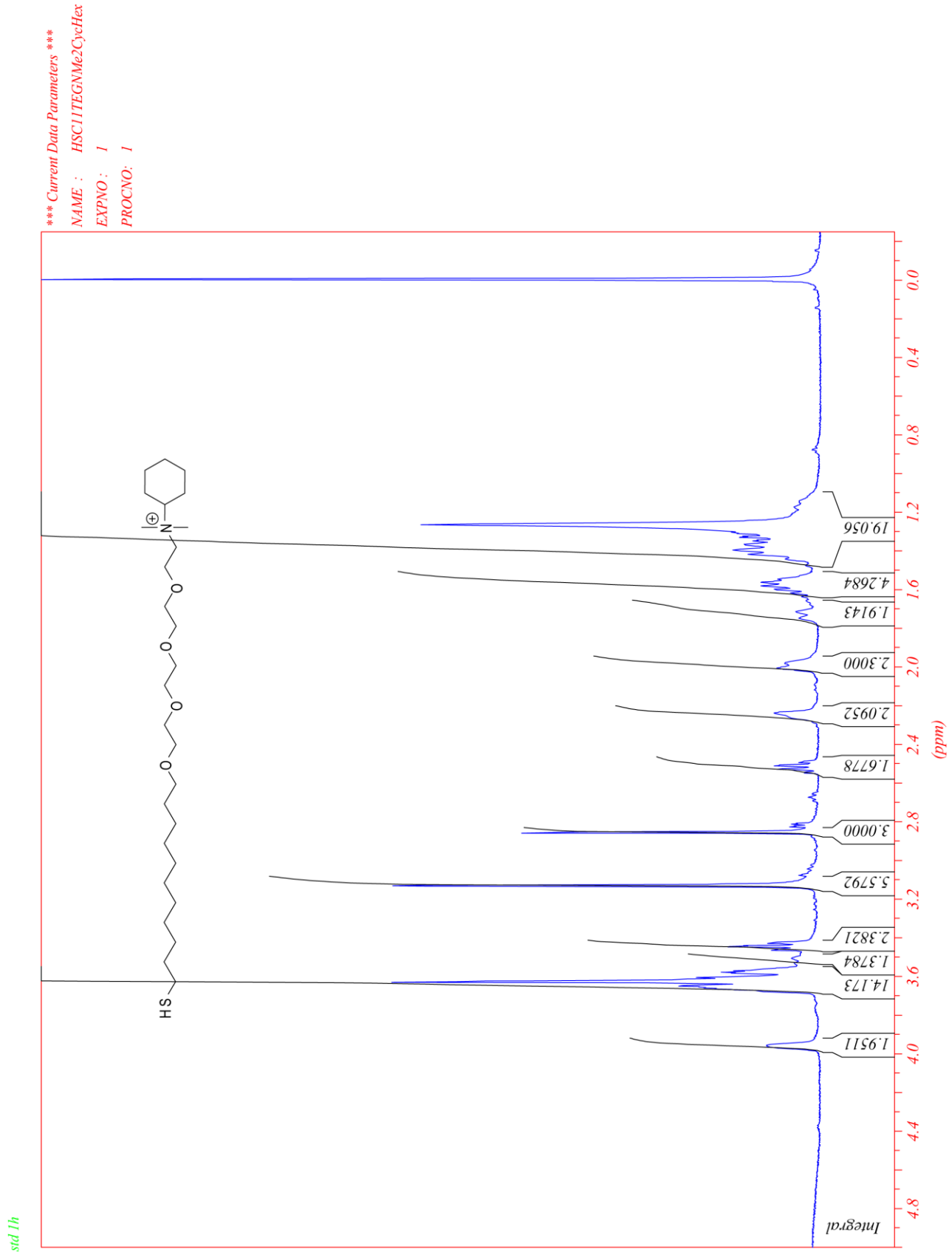

Figure S7. 400 MHz ^{1}H NMR spectra of **compound L2** in chloroform-D (D, 99.8%).

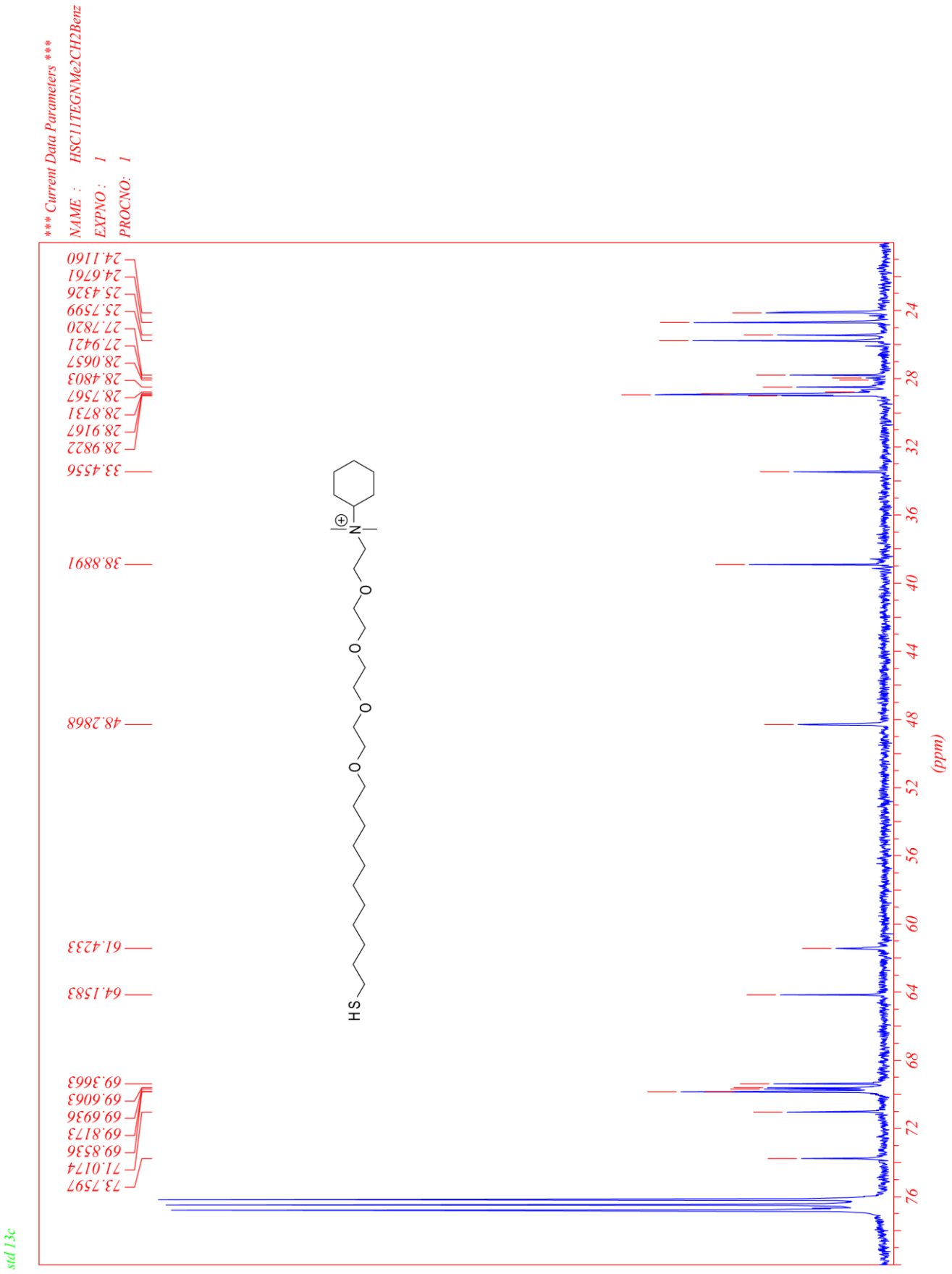

Figure S8. 400 MHz ^{13}C NMR spectra of **compound L2** in chloroform-D (D, 99.8%).

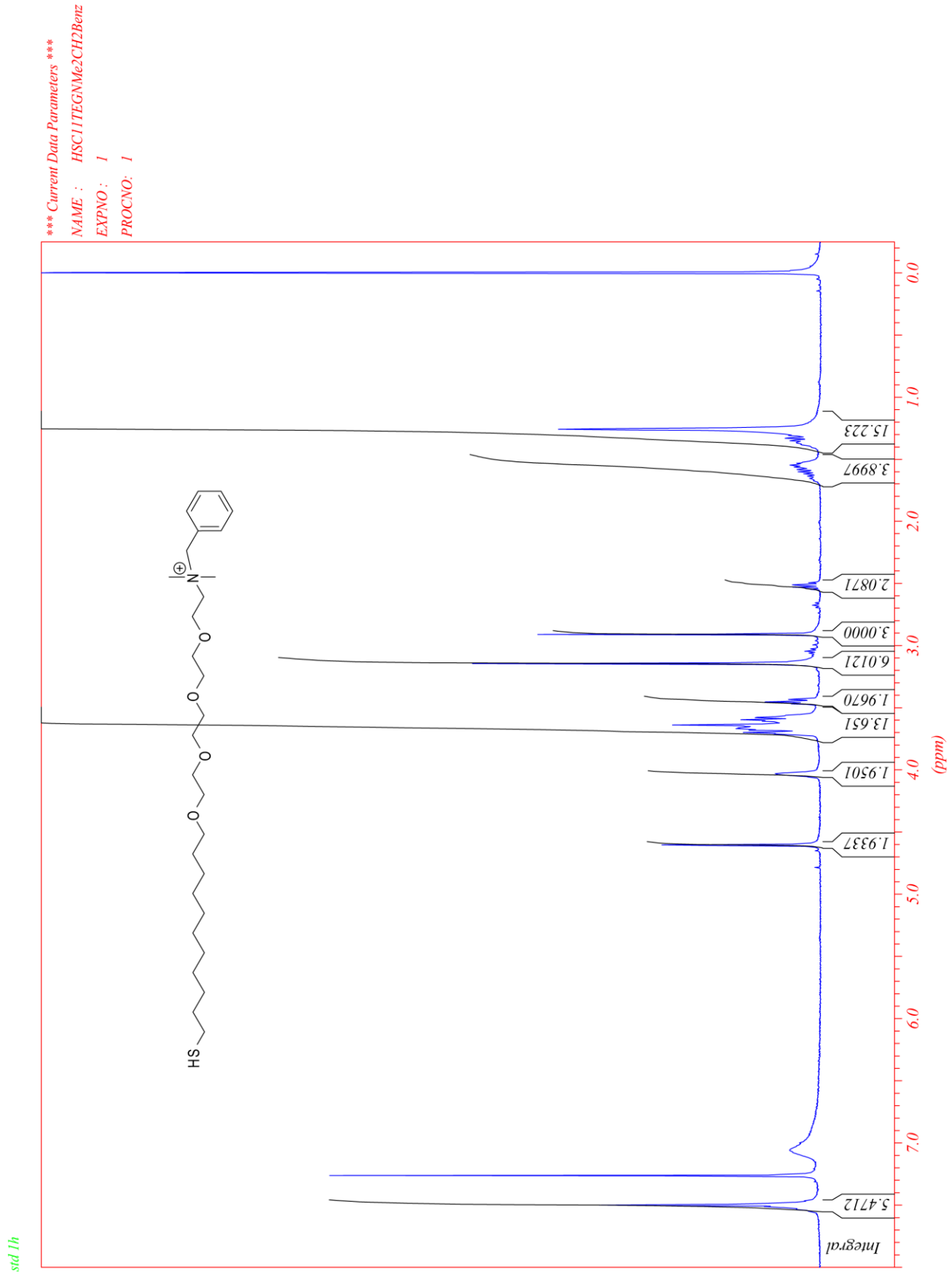

Figure S9. 400 MHz ^{1}H NMR spectra of **compound L3** in chloroform-D (D, 99.8%).

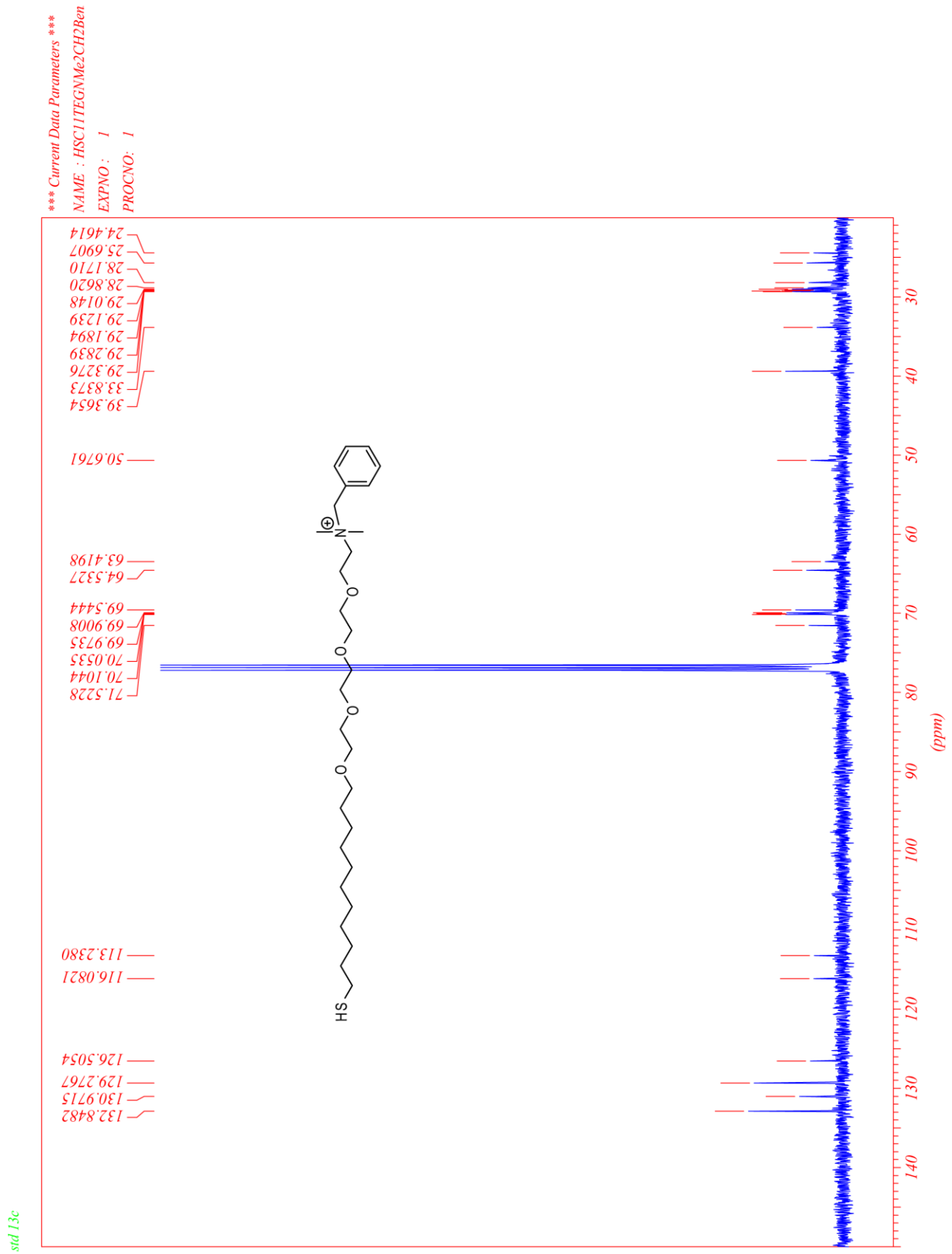

Figure S10. 400 MHz ^{13}C NMR spectra of **compound L3** in chloroform-D (D, 99.8%).

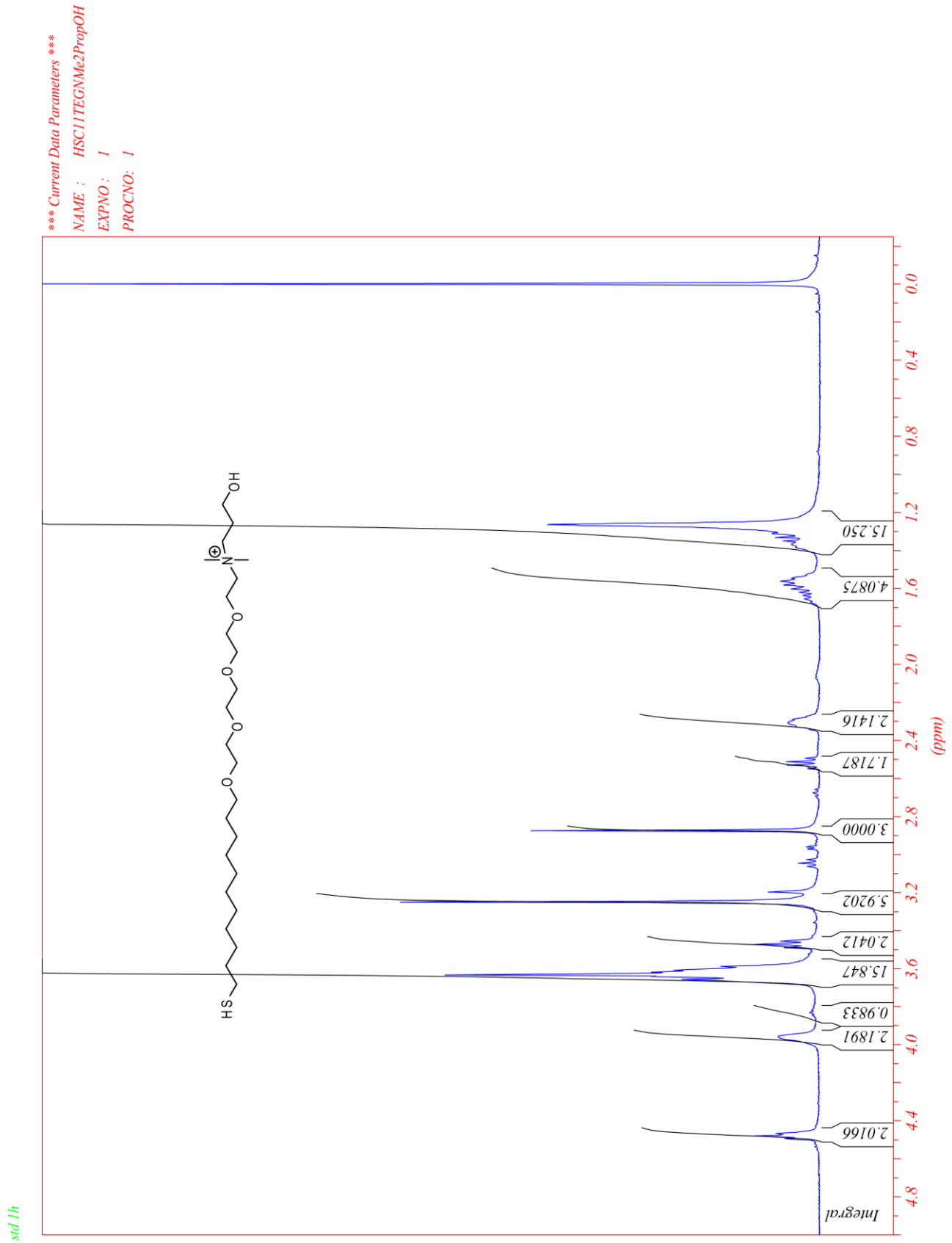

Figure S11. 400 MHz ^{1}H NMR spectra of **compound L4** in chloroform-D (D, 99.8%).

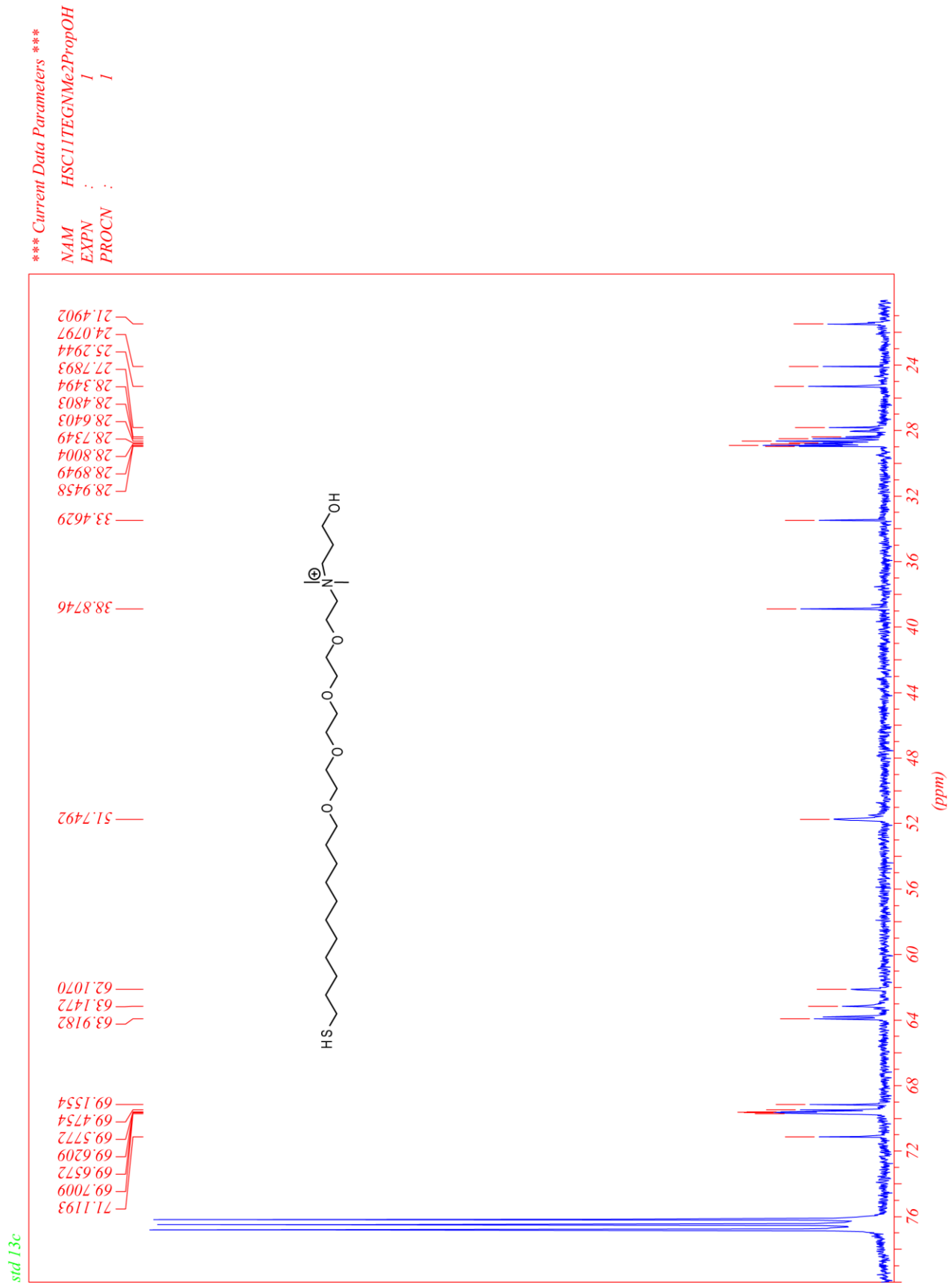

Figure S12. 400 MHz ^{13}C NMR spectra of **compound L4** in chloroform-D (D, 99.8%).

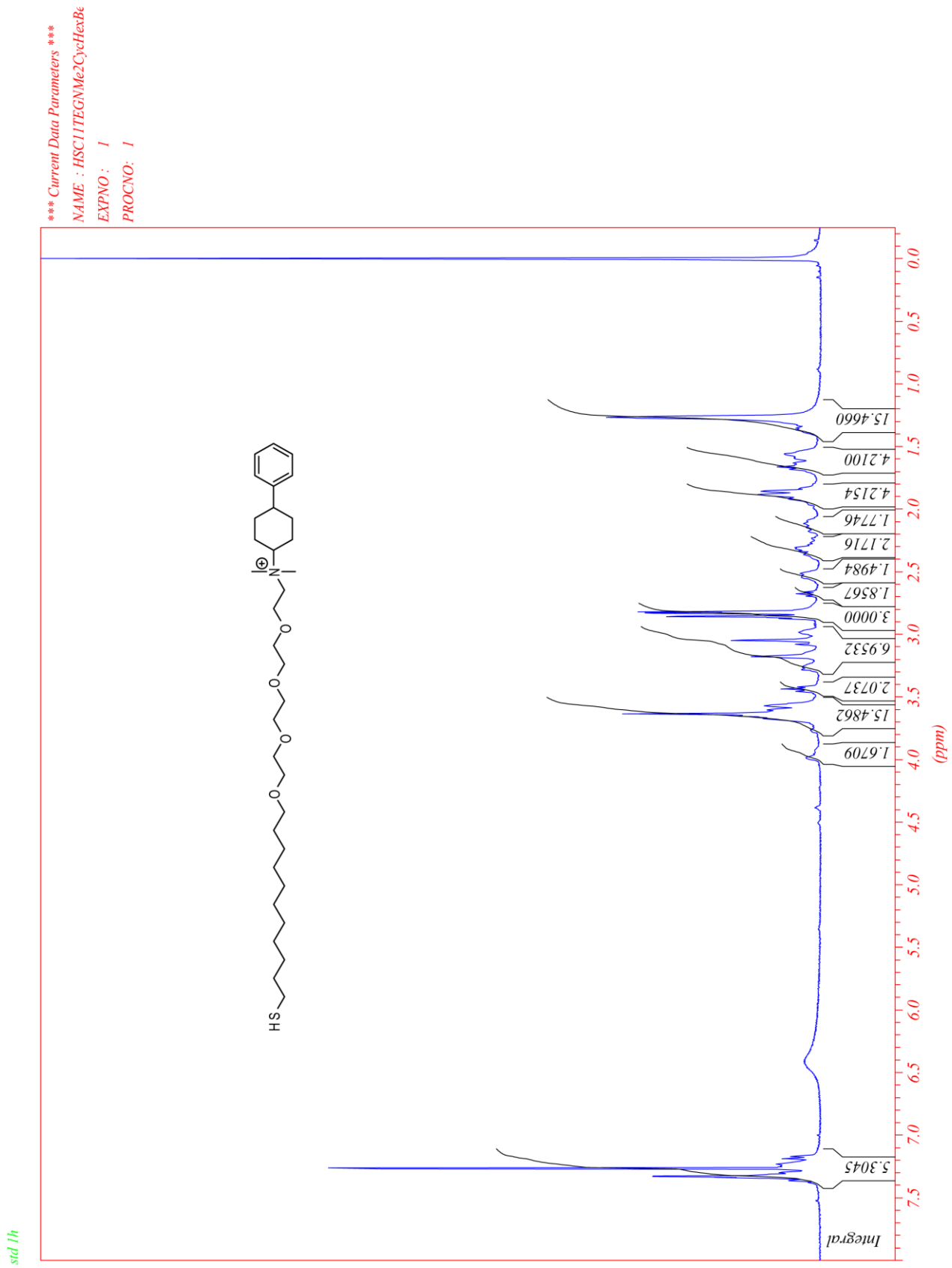

Figure S13. 400 MHz ^{1}H NMR spectra of **compound L5** in chloroform-D (D, 99.8%).

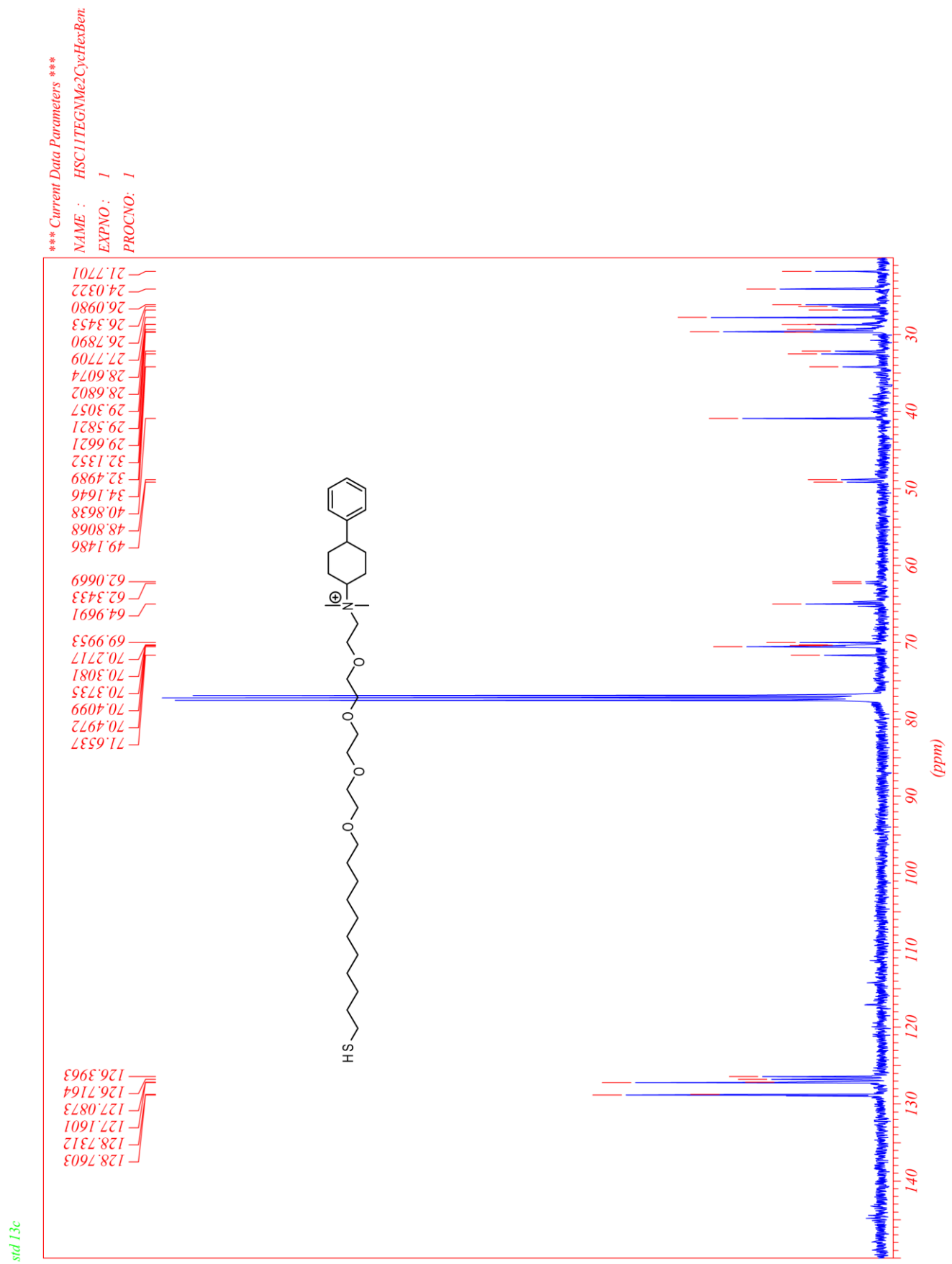

Figure S14. 400 MHz ^{13}C NMR spectra of **compound L5** in chloroform-D (D, 99.8%).

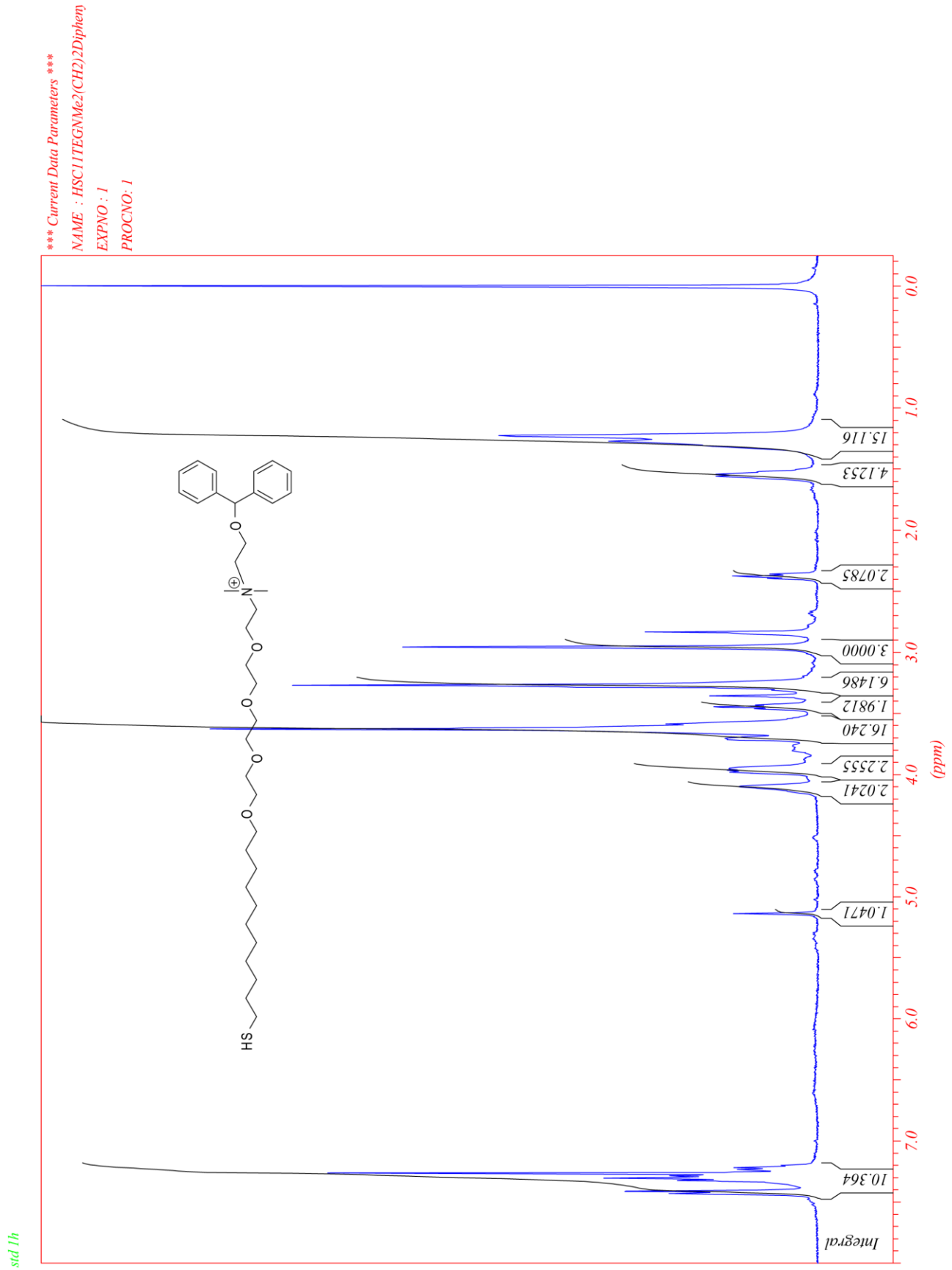

Figure S15. 400 MHz ^{1}H NMR spectra of **compound L6** in chloroform-D (D, 99.8%).

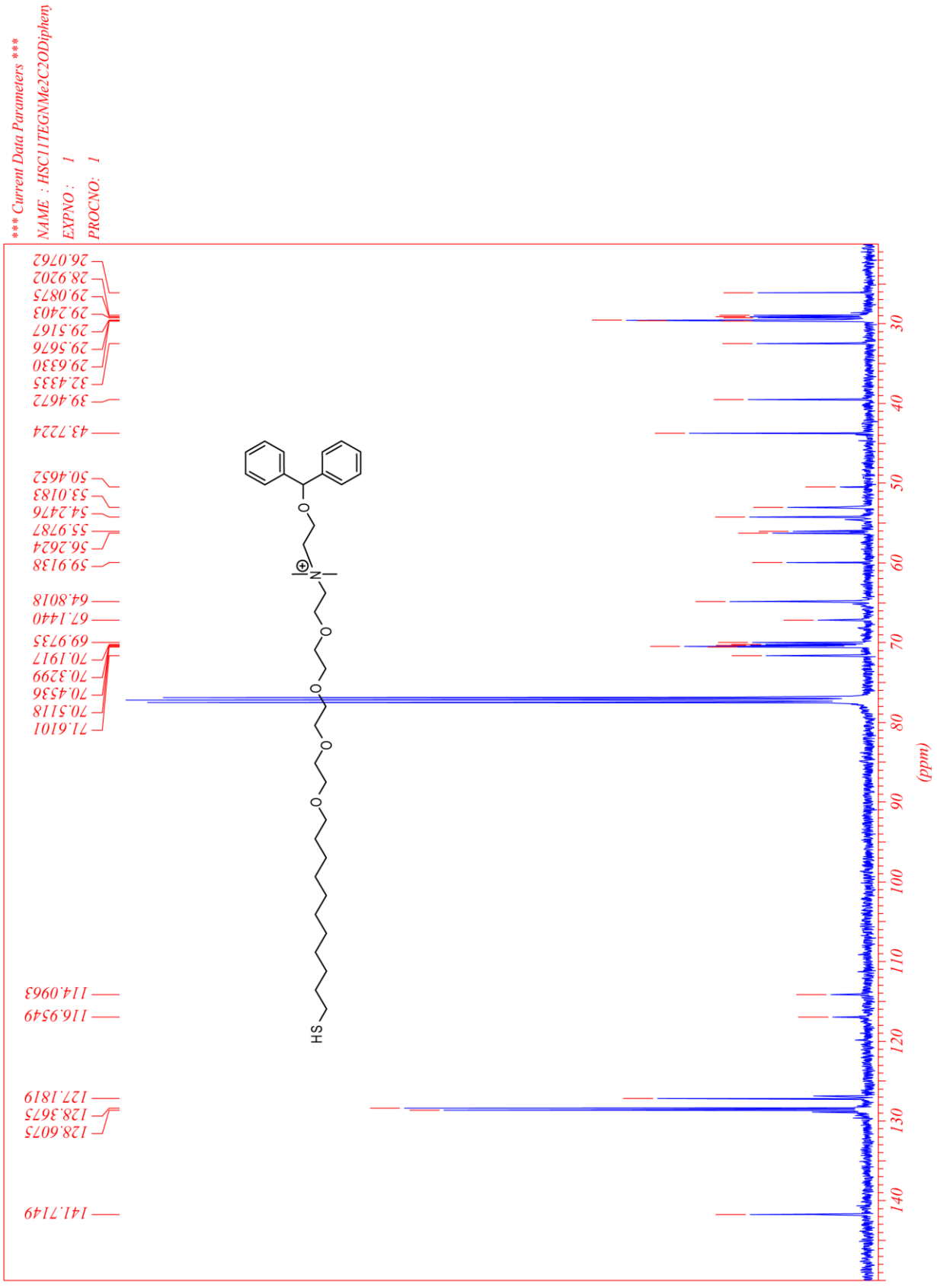

Figure S16. 400 MHz ^{13}C NMR spectra of **compound L6** in chloroform-D (D, 99.8%).

Scheme II. Synthesis of cationic gold nanoparticles **NP1-NP6.**

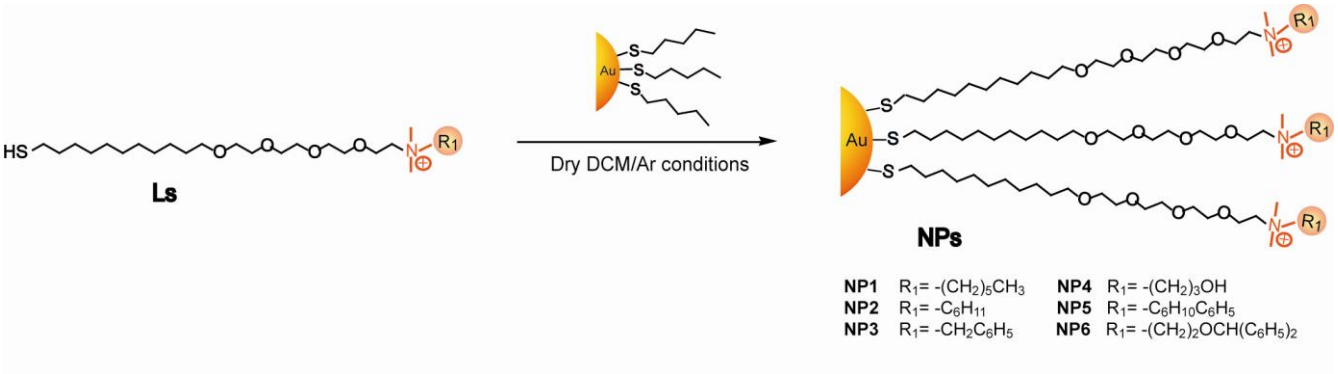

1-Pentanethiol coated gold nanoparticles (*d* = ~2 nm) were prepared according to the previously reported protocol (See NMR Figure S17).[4] A place-exchange reaction[5] of compound **Ls** dissolved in DCM with pentanethiol-coated gold nanoparticles (d~2 nm) was carried out for 3 days at room temperature. Then, DCM was evaporated under reduced pressure. The residue was dissolved in a small amount of distilled water and dialyzed (membrane MWCO = 1,000) to remove excess ligands, acetic acid and other salts present with the nanoparticles solution. After dialysis, the particles were lyophilized to obtain a brownish solid product. The particles (AuNPs) are redispersed in water and/or deionized water (18 MΩ-cm). ^{1}H NMR spectra in D_2O showed substantial broadening of the proton signals and no free ligands were observed (see Figures S18-S23).

[4] Brust, M.; Walker, M.; Bethell, D.; Schiffrin, D. J.; Whyman, R. *J. Chem. Soc., Chem. Commun.* **1994**, 801.

[5] Hostetler, M. J.; Templeton, A. C.; Murray, R. W. *Langmuir* **1999,** 15, 3782.

^{1}H NMR spectra of $AuS(CH_2)_4CH_3$

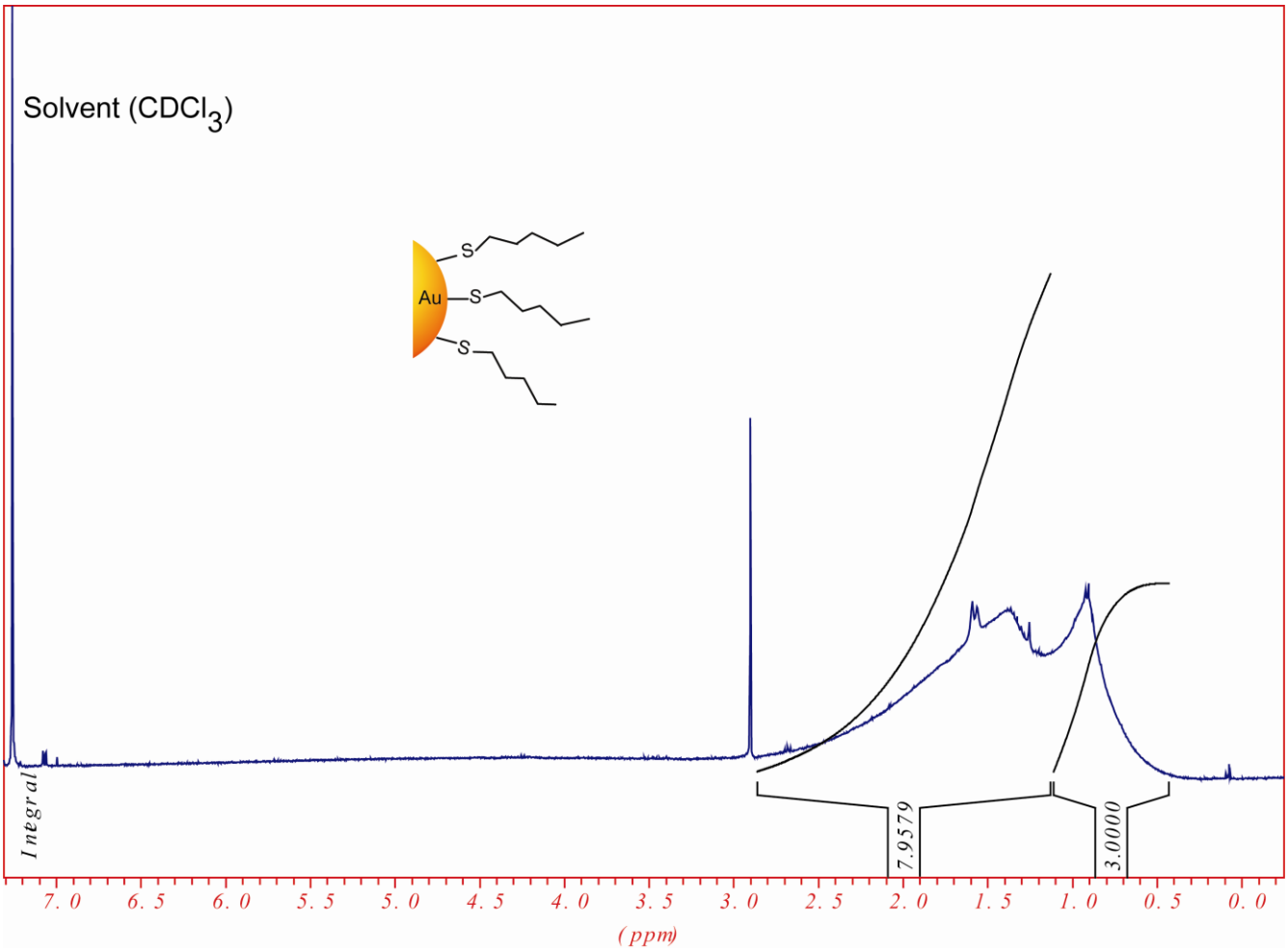

Figure S17. 400 MHz ^{1}H NMR of pentane-1-thiol capping the surface of the metal core gold nanoparticles. The average diameter of the metal core $AuS(CH_2)_4CH_3$ is ~ 2 nm (2.15 ± 0.31 nm).

^{1}H NMR spectra of **NP1** after place exchange with $AuS(CH_2)_4CH_3$

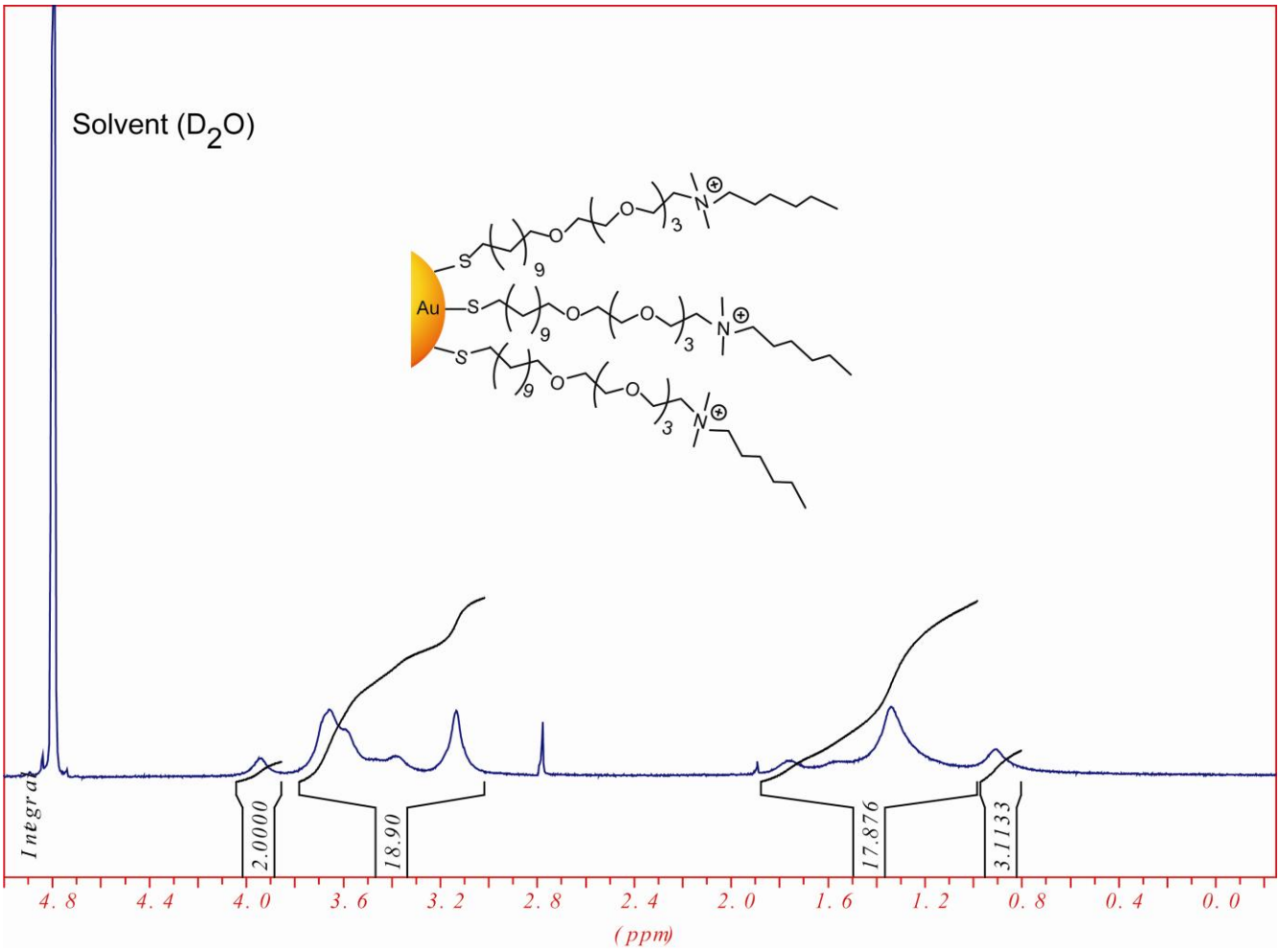

Figure S18. 400 MHz ^{1}H NMR of N-hexyl-23-mercapto-N,N-dimethyl-dimethyl-3,6,9, 12-tetraoxatricosan-1-aminium capping the surface of the metal core gold nanoparticles after place exchange. The average diameter of the metal core **NP1** is ~ 2 nm (2.15 ± 0.28 nm).

^{1}H NMR spectra of **NP2** after place exchange with $AuS(CH_2)_4CH_3$

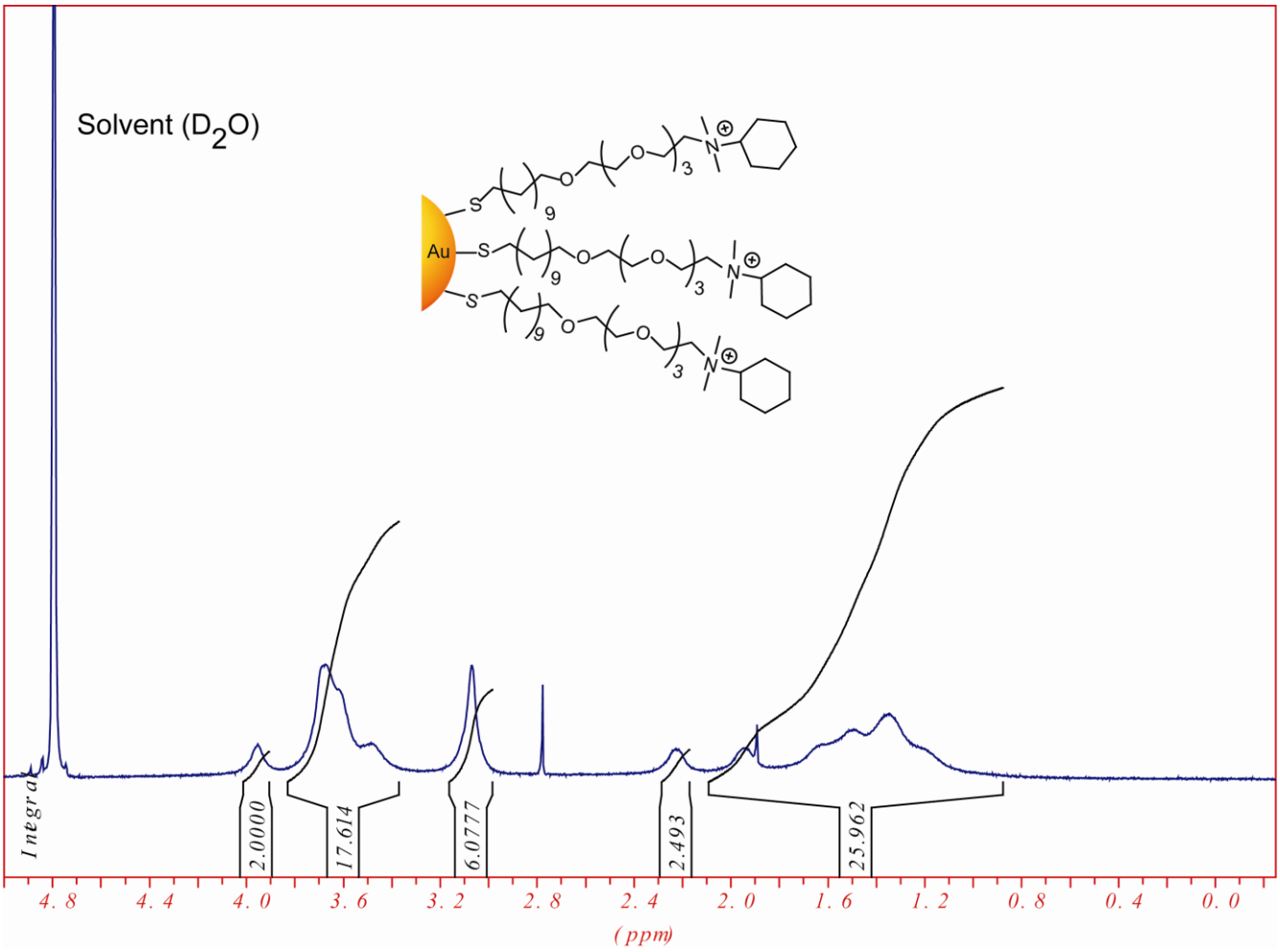

Figure S19. 400 MHz ^{1}H NMR of N-cyclohexyl-23-mercapto-N,N-dimethyl-3,6,9,12-tetraoxatricosan-1-aminium capping the surface of the metal core gold nanoparticles after place exchange. The average diameter of the metal core **NP2** is ~ 2 nm (2.09 ± 0.27 nm).

^{1}H NMR spectra of **NP3** after place exchange with $AuS(CH_2)_4CH_3$

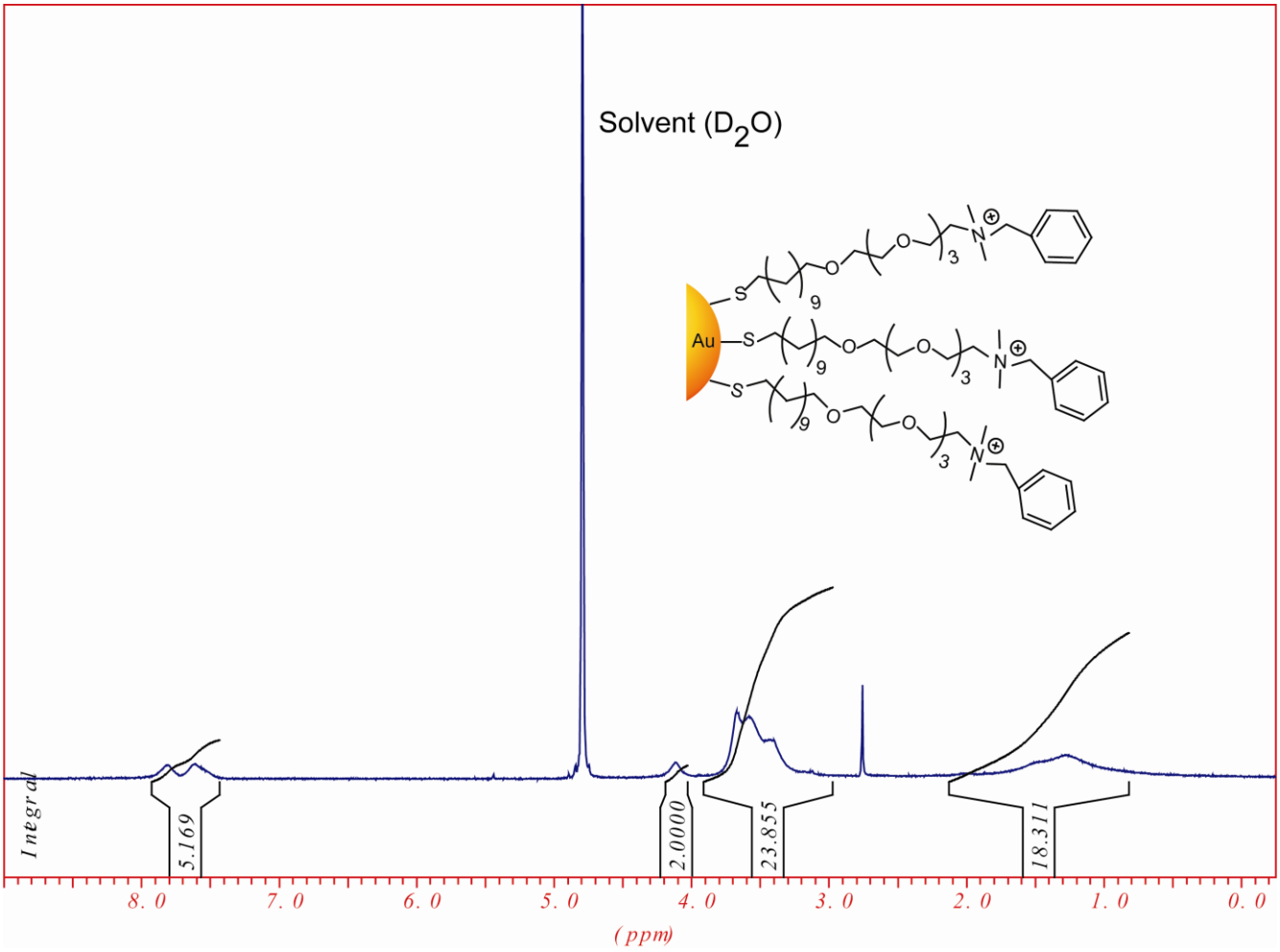

Figure S20. 400 MHz ^{1}H NMR of N-benzyl-23-mercapto-N,N-dimethyl-3,6,9,12-tetraoxatricosan-1-aminium capping the surface of the metal core gold nanoparticles after place exchange. The average diameter of the metal core **NP3** is ~ 2 nm (2.12 ± 0.21 nm).

^{1}H NMR spectra of **NP4** after place exchange with $AuS(CH_2)_4CH_3$

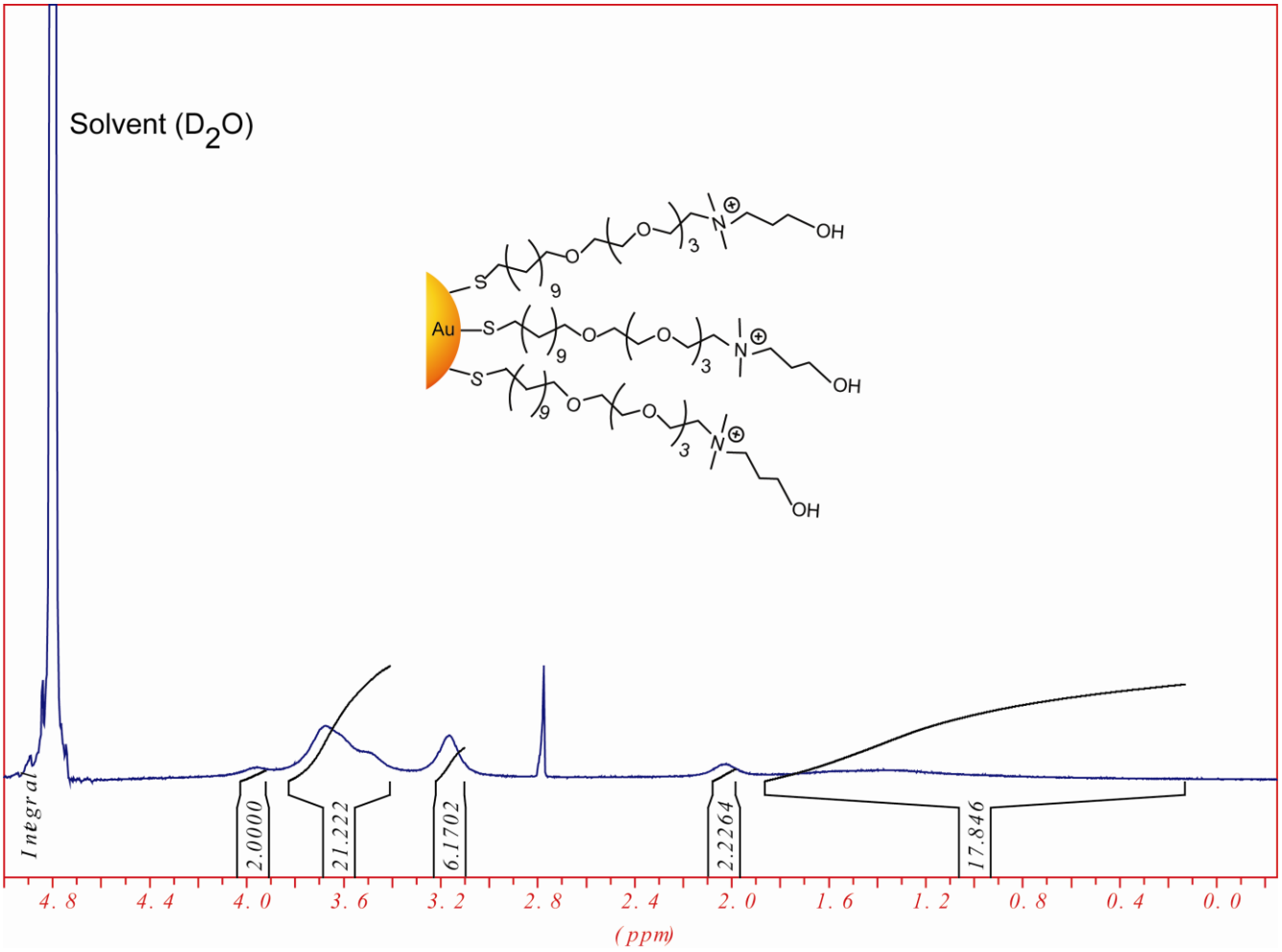

Figure S21. 400 MHz ^{1}H NMR of N-(3-hydroxypropyl)-23-mercapto-N,N-dimethyl-3,6,9,12-tetraoxatricosan-1-aminium capping the surface of the metal core gold nanoparticles after place exchange. The average diameter of the metal core **NP4** is ~ 2 nm (2.14 ± 0.25 nm).

^{1}H NMR spectra of **NP5** after place exchange with $AuS(CH_2)_4CH_3$

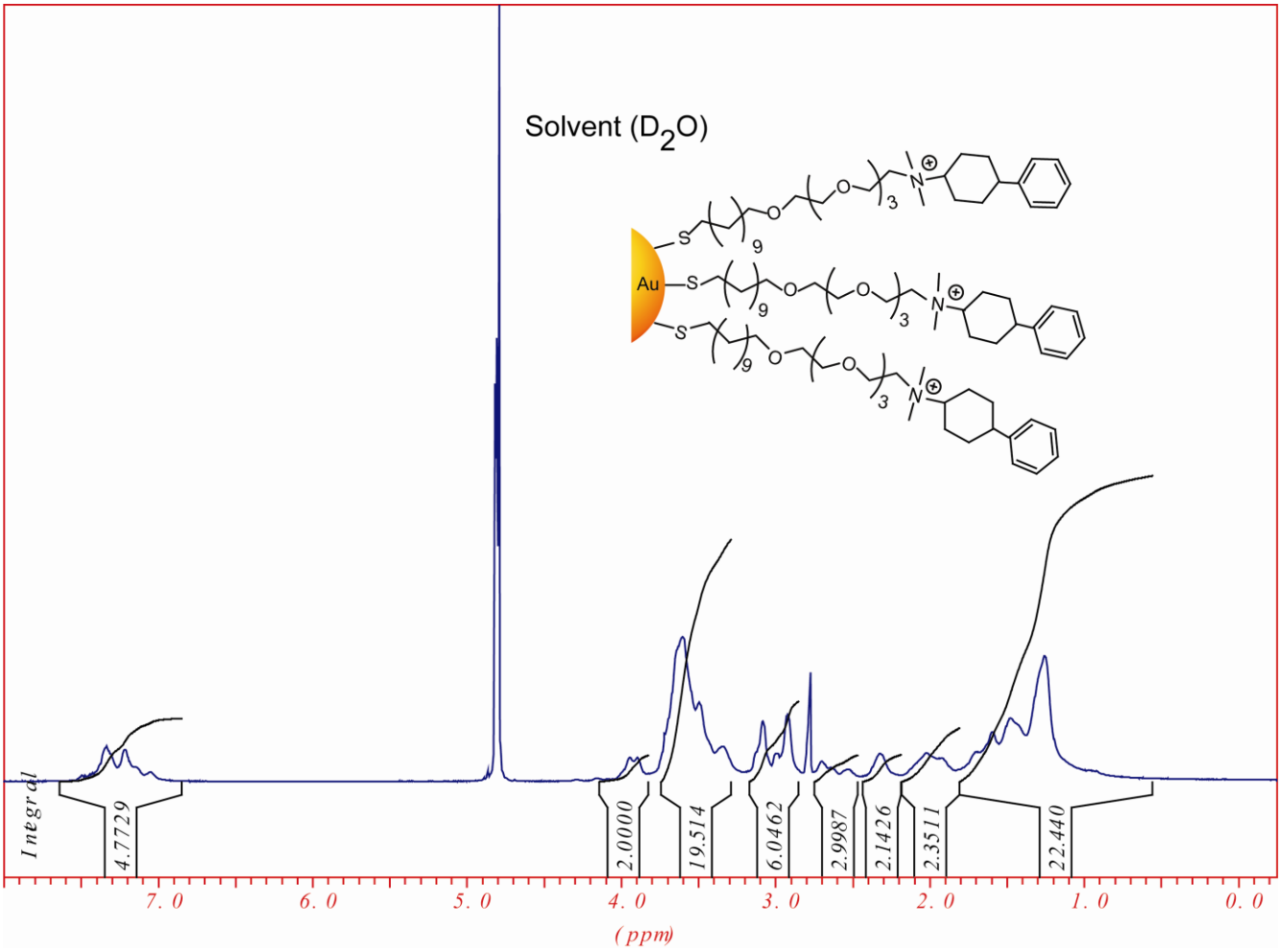

Figure S22. 400 MHz ^{1}H NMR of 23-mercapto-N,N-dimethyl-N-(4-phenylcyclohexyl)-3,6,9,12-tetraoxatricosan-1-aminium capping the surface of the metal core gold nanoparticles after place exchange. The average diameter of the metal core **NP5** is ~ 2 nm (2.10 ± 0.29 nm).

^{1}H NMR spectra of **NP6** after place exchange with $AuS(CH_2)_4CH_3$

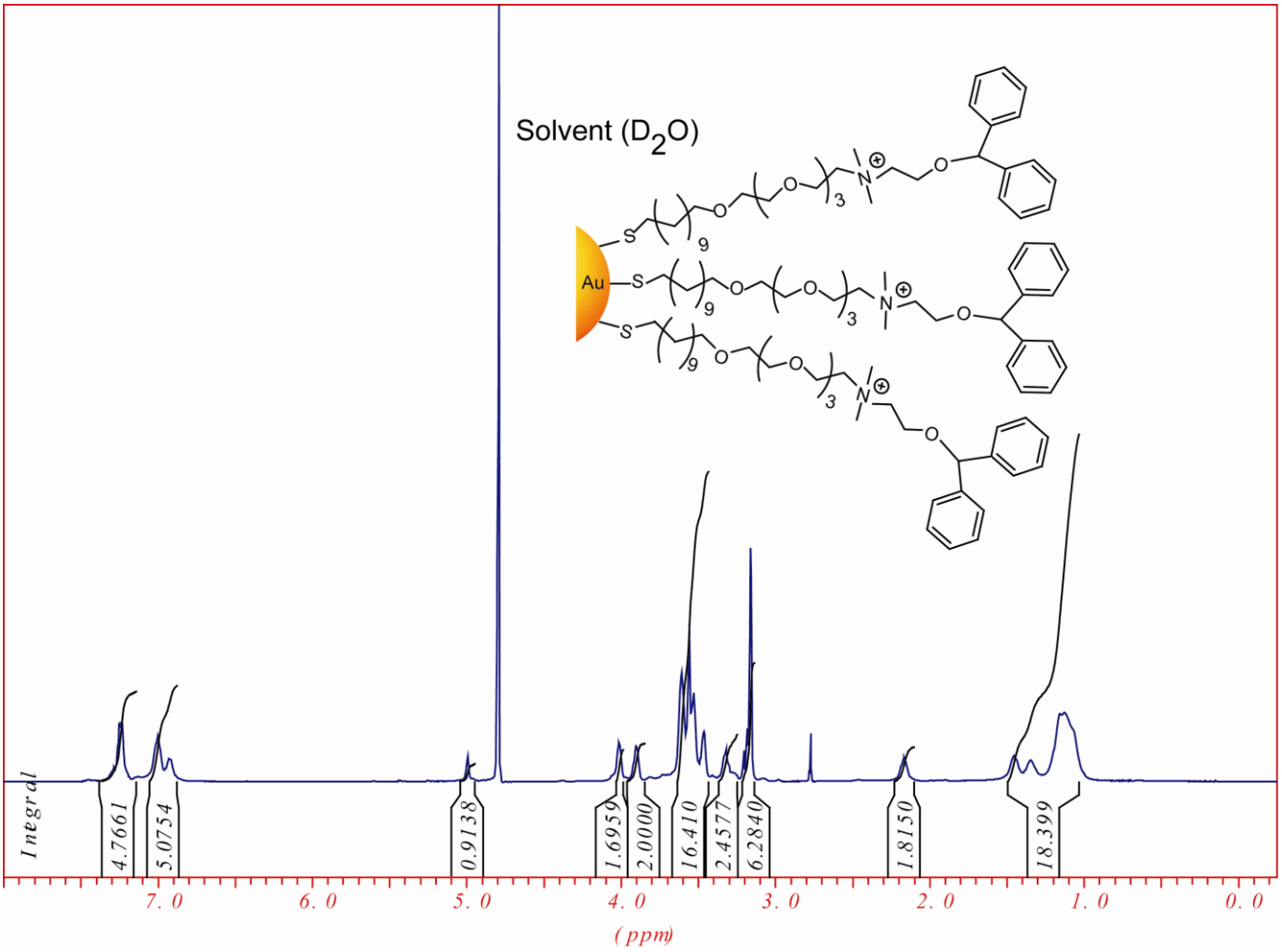

Figure S23. 400 MHz ^{1}H NMR of N-(2-(benzhydryloxy)ethyl)-23-mercapto-N,N-dimethyl-3,6,9,12-tetraoxatricosan-1-aminium capping the surface of the metal core gold nanoparticles after place exchange. The average diameter of the metal core **NP6** is ~ 2 nm (2.11 ± 0.22 nm)

Scheme III. Synthesis of tetraethylene glycol functionalized gold nanoparticles

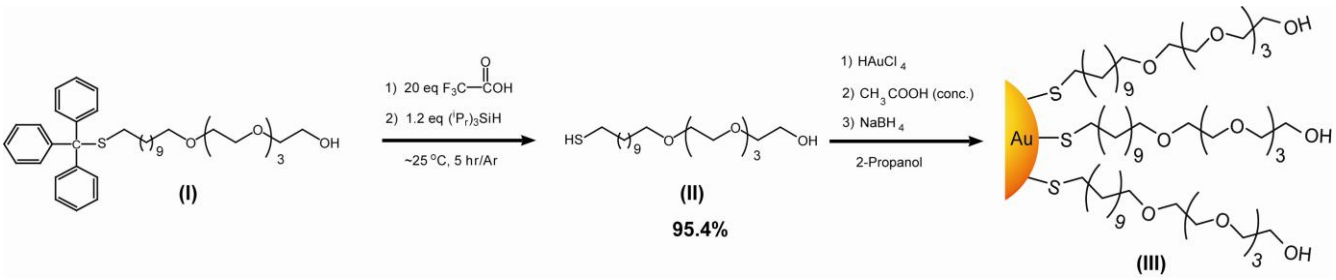

General procedure[6]**:** 60 mg of $HAuCl_4$ were dissolved in a mixture of 100 ml of 2-propanol and 1 ml of concentrated acetic acid (to prevent possible deprotonation of thiol molecules (**II**) after addition of excess $NaBH_4$). Compound **II** (Yield 4.57 g, >95.4%, see NMR Figure S24) bearing both thiols and hydroxyls end groups (monohydroxyl(1-mercaptounce-11-yl) was added under stirring conditions to the gold salt solution. $HAuCl_4$ was reduced by rapid addition of 10 ml of freshly prepared 0.5 M solution of $NaBH_4$ in methanol. The pale yellow gold solution turned black. After further stirring for 3 h, the volume of 2-propanol was reduced to 5-10 ml using a rotavapor. The synthesized AuNPs **(III, NP_{OH})** was precipitated by pouring the reaction mixture into hexane. The tetraethylene glycol functionalized particles were cleaned several times in hexane and were separated by centrifugation. ^1H NMR spectra in D_2O showed substantial broadening of the proton signals and no free ligands were observed (See NMR Figure S25). Please notes that compound (**I**) was synthesized as shown in scheme **I** (Yield 7.83 g, >65 %, see NMR Figure S3)**.**

[6] Kanaras, A. G.; Kamounah, F. S.; Schaumburg, K.; Kiely, Ch. J.; Brust, M. *Chem. Commun.* **2002**, 2294.

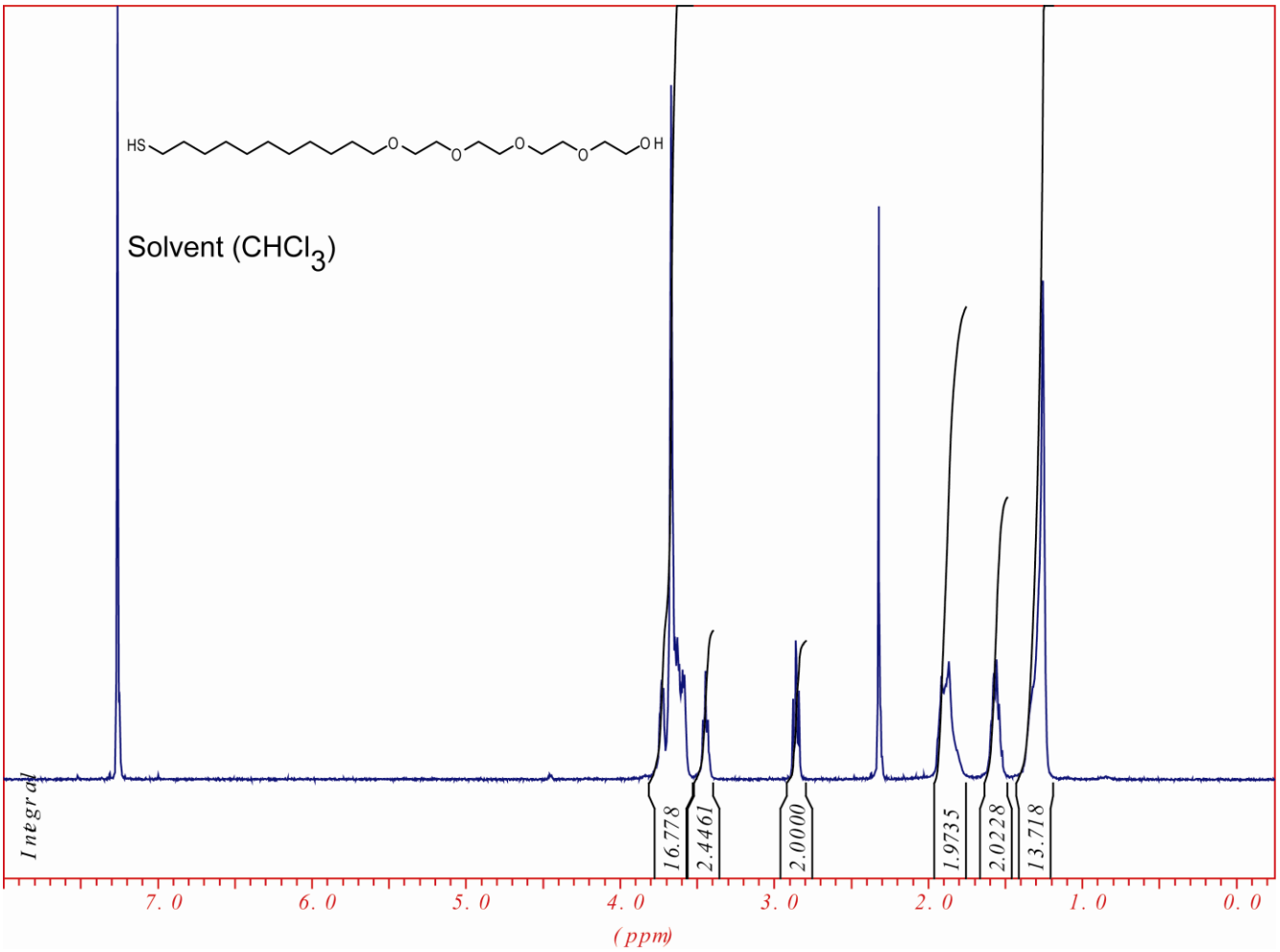

Figure S24. 400 MHz ^{1}H NMR spectra of **compound II** (23-mercapto-3,6,9,12-tetraoxatricosan-1-ol) in chloroform-D (D, 99.8%).

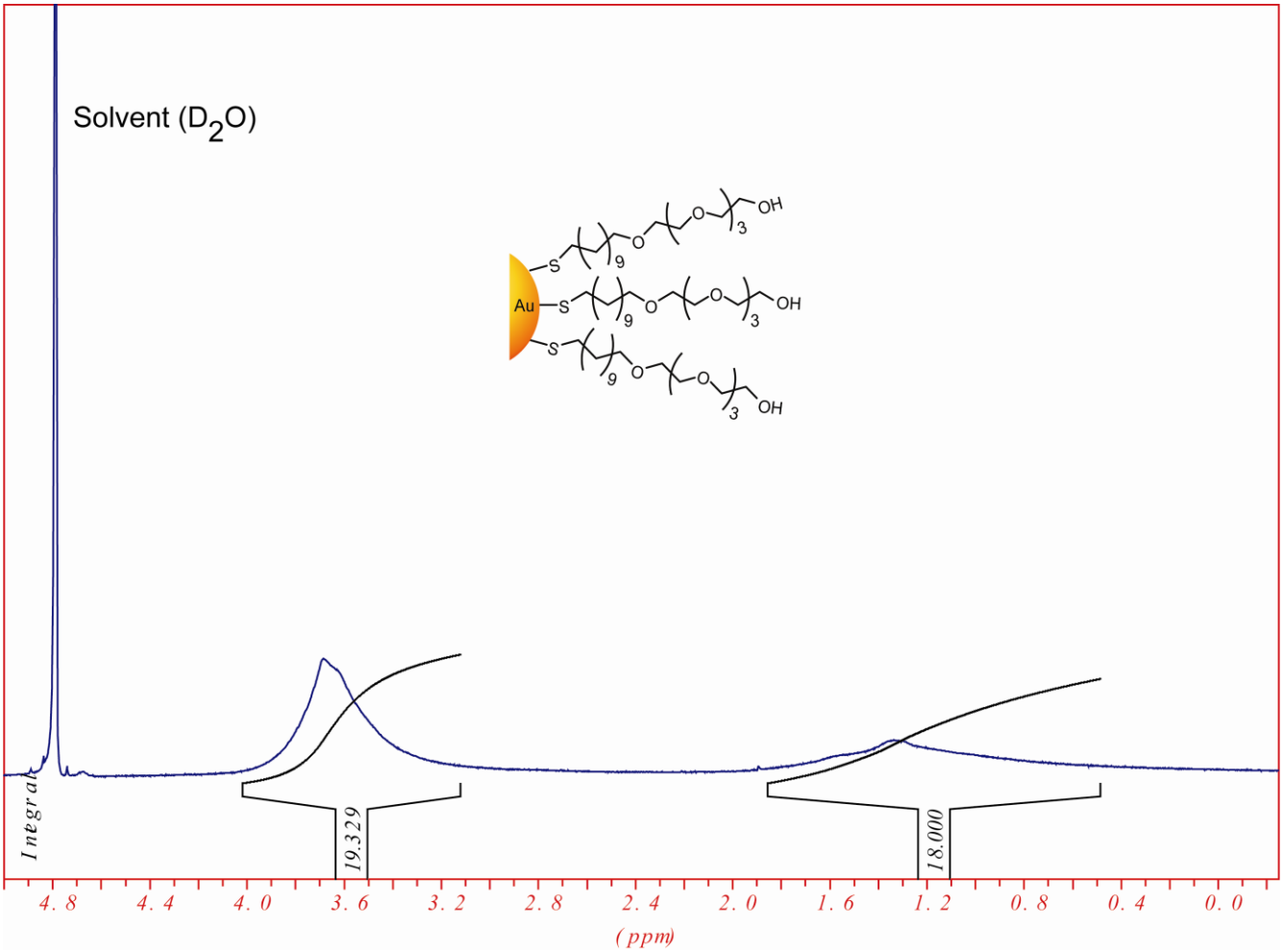

Figure S25. 400 MHz ^{1}H NMR of 23-mercapto-3,6,9,12-tetraoxatricosan-1-ol capping the surface of the metal core gold nanoparticles after synthesizing them. The average diameter of the metal core $\mathbf{NP_{OH}}$ is ~ 2 nm (2.40 ± 0.46 nm).

Figure S26. Fluorescence titration curves for the complexation of β-Gal with cationic gold nanoparticles (**NP1-NP6**). The inhibition study was measured following the addition of cationic nanoparticles (0-100 nM) with an excitation wavelength of 455 nm. The β-Gal stock concentration was 275 nM, while the stock concentration of **NP1-NP4** and **NP5-NP6** were 100 nM and 50 nM, respectively. For the activity/inhibition studies, optimal concentrations of β-Gal/AuNP complexes were obtained (β-Gal = 0.5 nM and **NP1**: 14 nM, **NP2**: 5 nM, **NP3**: 6 nM, **NP4**: 32 nM, **NP5**: 6 nM and **NP6**: 10 nM)

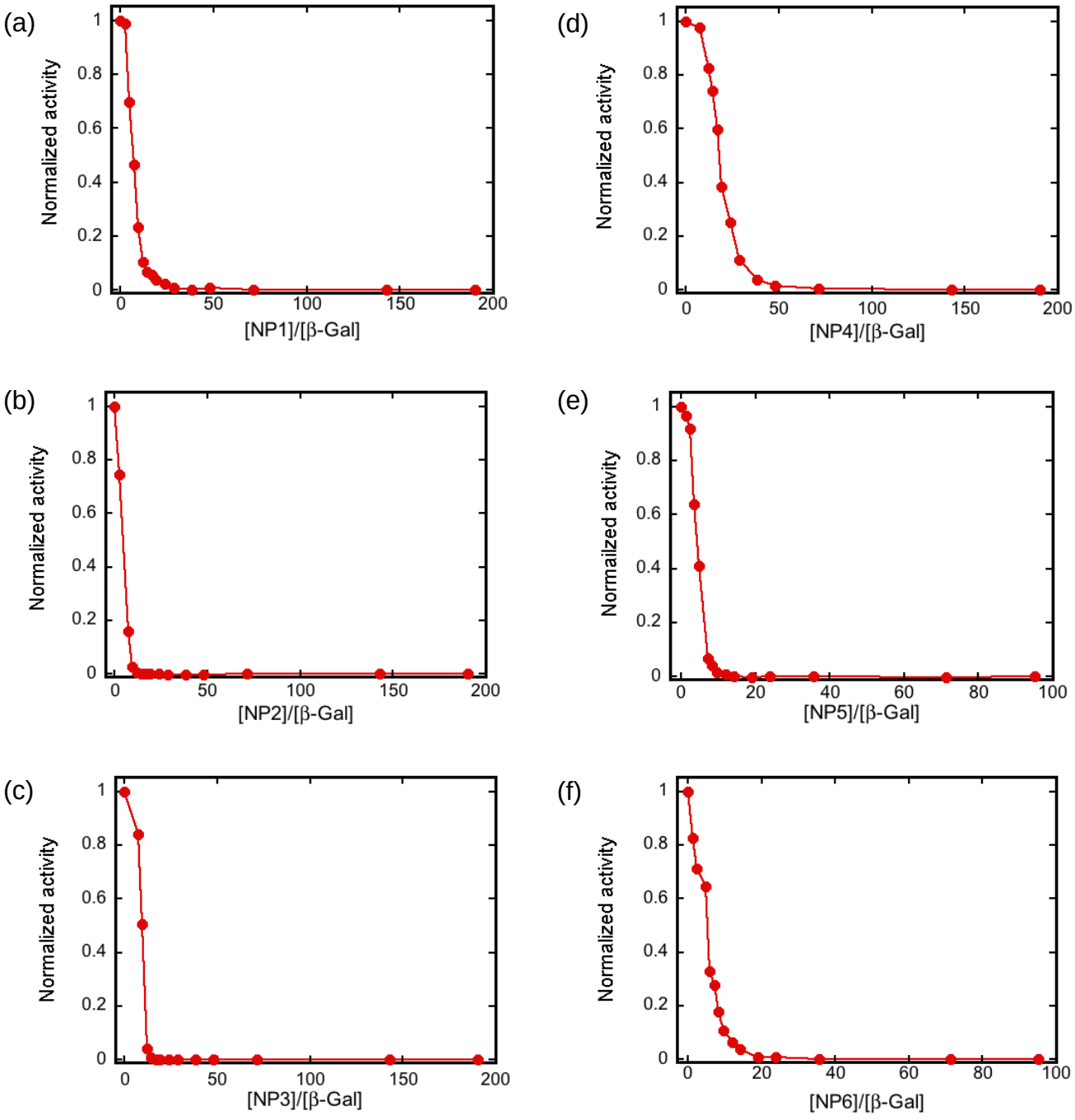

Table S1. Final and initial kinetics ratio of the fluorescence response patterns of β-Gal and six AuNPs (**NP1**-**NP6**) adducts against various target proteins ± the standard deviation (SD). Each value represents an average of six parallel measurements.

Proteins	($V_{max}/V_{o,max}$)											
	NP1	***SD***	***NP2***	***SD***	***NP3***	***SD***	***NP4***	***SD***	***NP5***	***SD***	***NP6***	***SD***
α-Amy	1.032631	0.023070	49.826124	5.782580	2.521877	0.642766	0.956224	0.065155	1.605185	0.236992	3.685843	0.410927
BSA	0.999694	0.021073	5.495259	1.192272	3.563111	1.135221	4.621077	1.189828	3.189334	1.045792	4.400572	2.060501
CytC	1.099279	0.038270	7.035717	1.641028	4.688597	0.888432	1.047342	0.056569	3.059661	0.815755	3.247085	0.923202
Fer	0.992357	0.013876	5.907556	1.403126	1.248837	0.077110	1.049945	0.240083	3.939724	1.574754	4.814340	1.156489
HSA	1.022090	0.093190	0.578550	0.061970	0.593520	0.082680	1.053750	0.020060	0.198600	0.078690	1.067530	0.030660
Lip	1.016972	0.022431	21.891588	7.816683	7.545811	1.491518	1.048292	0.028982	5.889066	2.165569	12.169190	1.601643
Lys	1.033740	0.032185	25.554471	3.995886	2.064363	0.457939	1.033634	0.024631	1.208252	0.108581	7.644296	0.648020
Myo	0.949131	0.028495	6.355809	2.647767	2.795169	1.091327	1.008620	0.023961	2.446874	0.481337	7.567806	1.130111
PhosB	1.082503	0.045996	9.308256	3.585956	7.184626	1.906531	1.051838	0.048903	1.643739	0.450590	7.773445	0.881225

Table S2. Training matrix of activity response patterns generated from β-Gal/AuNP sensor array (**NP1**–**NP6**) and the fluorogenic substrate (4-Methylumbelliferyl-beta-D-galactopyranoside) against various types of proteins (concentration = 1 nM)

Protein	**NP1**	**NP2**	**NP3**	**NP4**	**NP5**	**NP6**
BSA	0.044053	3.214873	1.915919	3.019801	1.508394	2.596625
BSA	0.001803	2.751742	1.862452	2.7310954	1.929778	2.125469
BSA	-0.029208	5.238646	4.532112	6.1428905	4.079058	8.703043
BSA	-0.005562	5.150131	2.309229	4.3265513	1.57304	2.363229
BSA	-0.002474	3.970872	1.487962	3.064843	3.281544	4.358388
BSA	-0.010731	5.38278	2.692894	4.6892543	1.484737	4.295396
α-Amy	0.030533	47.949173	2.694459	0.04751	0.971899	4.085935
α-Amy	0.030473	40.106219	1.095875	0.024666	0.872635	3.451511
α-Amy	0.037562	49.668787	1.225475	-0.038449	0.568434	3.20844
α-Amy	0.046226	48.437045	1.068158	-0.08928	0.49703	2.897434
α-Amy	-0.000473	53.43828	1.464148	-0.123741	0.289909	2.854269
α-Amy	0.081295	39.644225	1.239895	-0.110541	0.630381	2.807335
PhosB	0.026263	5.167704	5.097584	0.031897	0.506591	9.209252
PhosB	0.085332	8.328736	7.486119	0.129765	0.59378	7.720325
PhosB	0.091886	5.566015	8.598139	-0.00099	1.499621	8.635416
PhosB	0.170683	8.147285	3.929951	0.010107	0.340704	6.876555
PhosB	0.099291	13.73013	6.251962	0.077694	0.397096	9.220521
PhosB	0.096983	6.576261	4.349083	0.094739	0.736506	7.02314
Myo	-0.033206	8.080209	2.630773	0.021627	2.082037	6.037168
Myo	-0.027848	4.615996	1.559139	0.044039	1.226572	7.504394
Myo	-0.033647	7.094949	2.565082	0.006033	2.241766	9.31948
Myo	-0.103298	5.823526	2.629196	0.006574	1.203914	9.472293
Myo	-0.060838	4.055951	0.713224	0.015152	1.29802	7.997081
Myo	-0.09288	0.960021	0.268708	-0.036356	1.105129	6.876726
HSA	0.034241	11.695738	0.117799	0.01436	0.210229	9.729707
HSA	0.030275	16.082641	0.27824	-0.000932	0.175173	12.303557
HSA	0.030139	9.63946	0.161239	0.033209	0.13621	12.761519
HSA	0.000204	14.385132	0.165391	0.013896	0.132509	13.612848
HSA	-0.040128	14.886227	0.246951	0.035259	0.184369	11.848571
HSA	-0.070378	11.715753	0.156712	-0.001143	0.183518	11.504987

CytC	0.184217	3.334292	2.484168	0.00432	1.997726	3.585885
CytC	0.086233	6.881454	3.775898	0.058127	2.035972	3.80381
CytC	0.093745	6.705778	2.958707	0.162795	1.009177	1.514039
CytC	0.133485	4.480754	4.809584	0.022029	2.466796	2.025927
CytC	0.059278	7.360435	3.126939	0.037145	1.892558	3.668159
CytC	0.129476	5.756436	4.144335	0.029029	3.633607	1.553461
Lip	0.03489	15.975745	6.129009	0.044412	3.649662	12.760949
Lip	-0.006349	14.685047	5.771155	0.049339	4.351439	11.519174
Lip	0.059929	23.193191	7.965504	0.044512	7.374255	13.884153
Lip	0.016398	33.350164	7.693391	0.116974	2.994633	14.215449
Lip	-0.008592	18.87153	6.235977	0.033004	3.938793	11.4049
Lip	0.02107	13.406363	4.003451	0.03149	8.634694	16.495692
Fer	0.015638	3.881425	0.250667	0.594025	0.91143	4.736998
Fer	-0.025041	3.76365	0.194659	-0.079998	2.743015	5.65528
Fer	-0.012179	6.219136	0.175432	-0.055006	2.912148	5.733982
Fer	-0.001526	4.868176	0.352427	-0.020403	5.77607	5.321418
Fer	-0.026687	6.258195	0.181103	-0.036432	4.048367	3.833469
Fer	-0.003048	3.076446	0.282612	-0.071511	2.21483	2.135025
Lys	0.039216	18.908905	1.43748	0.02018	0.35339	8.155539
Lys	0.021889	25.932638	1.674801	0.087391	0.089727	8.739942
Lys	0.02705	23.321727	0.795414	0.033402	0.252776	6.517422
Lys	-0.011735	18.721133	0.953478	0.037755	0.091089	8.167482
Lys	0.058959	25.967241	0.523449	0.007717	0.198486	7.764536
Lys	0.097906	27.578963	0.761495	0.036241	0.332586	8.412007

Table S3. Accuracy of LDA classification of protein analytes (Conc. = 1 nM) from the complexes of the enzyme (β-Gal) with individual cationic nanoparticles as sensors. The values are taken from the Jackknifed classification matrix based on LDA analysis of the raw data (6 replicates) listed in Table S1.

Protein	**NP1-** (β-Gal)	**NP2-** (β-Gal)	**NP3-** (β-Gal)	**NP4-** (β-Gal)	**NP5-** (β-Gal)	**NP6-** (β-Gal)
α-Amy	17%	100%	17%	67%	50%	33%
BSA	17%	50%	33%	100%	0%	17%
CytC	50%	33%	50%	0%	50%	50%
Fer	50%	17%	50%	0%	33%	67%
HSA	0%	83%	67%	33%	83%	50%
Lip	33%	17%	50%	0%	50%	67%
Lys	17%	67%	50%	50%	67%	0%
Myo	50%	0%	0%	33%	50%	17%
PhosB	67%	33%	17%	0%	17%	17%
Total	33%	44%	37%	31%	44%	35%

Table S4. Identification of 60 unknowns protein samples with LDA using β-Gal/AuNP sensor array.

Entry	Fluorescence response pattern						Identification	Accuracy
	NP1- (β-Gal)	**NP2-** (β-Gal)	**NP3-** (β-Gal)	**NP4-** (β-Gal)	**NP5-** (β-Gal)	**NP6-** (β-Gal)	Proteins	YES/NO
1	0.0249	5.0111	7.0148	0.0265	7.7240	6.0431	PhosB	YES
2	-0.0319	7.0499	1.0191	0.0454	2.0664	7.9505	Myo	YES
3	-0.0241	4.0722	0.2621	-0.0477	3.5312	2.8284	Fer	YES
4	0.0432	19.0053	0.9033	0.0577	0.3114	6.2252	Lys	YES
5	0.0482	42.0235	2.0051	-0.1494	0.9479	2.6495	Amy	YES
6	-0.0532	20.0375	7.0020	0.0513	5.0730	14.7841	Lip	YES

7	-0.1396	4.0600	3.0306	0.0184	3.5895	2.9529	CytC	YES
8	-0.0477	10.1205	0.1779	-0.0306	0.1808	11.3290	HSA	YES
9	0.0490	22.0385	1.0080	0.0366	0.2627	7.9681	Lys	YES
10	-0.0159	3.0547	0.0240	-0.0401	2.4212	5.2937	Fer	YES
11	-0.0519	27.0321	6.0071	0.0481	5.1727	12.4804	Lip	YES
12	0.0406	6.0647	4.0280	0.0505	1.3679	7.6684	PhosB	YES
13	-0.0690	27.0339	7.0287	0.0546	4.0528	13.9802	Lip	YES
14	0.0669	25.0304	0.9457	0.0471	0.1769	8.4429	Lys	YES
15	0.0235	14.0188	0.2401	0.1601	0.1327	12.9316	HSA	YES
16	-0.0725	8.0147	1.0279	0.0063	1.6280	9.0444	Myo	YES
17	0.0947	5.0075	4.0441	0.0454	2.0443	2.8999	CytC	YES
18	0.0653	7.0399	3.1420	0.0542	1.6320	1.6501	Fer	NO
19	-0.0368	11.1823	0.1548	0.0364	0.2355	11.8070	HSA	YES
20	0.1032	4.0846	2.9033	0.0637	2.1633	1.9459	CytC	YES
21	0.0270	8.0277	4.3149	-0.0027	0.7895	7.4108	PhosB	YES
22	-0.0127	50.0125	2.0083	-0.0249	0.2990	2.6078	Amy	YES
23	0.0173	5.0105	3.0119	0.0290	2.3539	1.0394	CytC	YES
24	-0.0205	8.0175	2.0432	0.0410	1.5333	9.0862	Myo	YES
25	-0.0082	13.0109	0.2192	-0.0301	0.1516	11.8710	HSA	YES
26	0.0248	20.0153	7.0042	0.7316	5.4685	13.0649	Lip	NO
27	-0.0128	44.0447	1.8053	0.0241	4.2127	7.1356	Amy	YES
28	0.0985	8.1151	6.0505	0.1189	0.8590	6.8917	PhosB	YES
29	-0.0338	3.0126	1.0091	5.0363	1.5770	2.1641	BSA	YES
30	-0.0114	45.0051	1.0187	-0.0367	0.7776	2.5967	Amy	YES
31	-0.0702	0.0299	-0.1050	-0.0455	2.4480	2.2238	Fer	NO
32	-0.0356	13.1249	0.2015	-0.0542	0.1703	12.8905	HSA	YES
33	-0.0261	6.0661	0.3170	-0.0571	2.8549	4.5573	Fer	YES
34	-0.0291	5.1087	2.0284	-0.0303	1.6971	6.5164	Myo	YES
35	0.1081	4.4278	3.0256	0.0358	3.0605	1.9780	CytC	YES
36	-0.0332	0.2987	0.0992	-0.0133	8.2027	6.8927	Fer	YES
37	0.0514	2.8060	4.8809	6.0245	2.1747	8.1074	BSA	YES
38	0.1259	6.0918	3.9306	0.0217	1.4871	2.1888	CytC	YES
39	-0.0205	26.1369	5.5155	0.0530	4.1899	7.7610	Lys	YES
40	0.2482	21.5107	0.8112	0.0423	0.2183	14.3341	Lip	YES
41	-0.0620	7.7939	0.4299	0.0339	1.8662	6.7561	Fer	NO
42	0.3158	15.3109	0.2225	-0.0416	0.2131	14.1598	Lip	NO
43	0.0208	19.9544	6.2423	0.0622	7.4915	15.0587	Lip	YES
44	0.0391	26.8454	1.5656	0.0363	0.2279	7.7122	Lys	YES
45	0.0373	48.5690	2.0407	0.0460	0.9108	3.7984	Amy	YES
46	0.0305	3.2047	1.4620	3.0280	1.6631	2.9823	BSA	YES
47	0.0399	23.0935	1.0030	0.0393	0.3487	7.8088	Lys	YES
48	-0.0232	4.0325	0.0346	-0.0316	2.5385	5.0346	Fer	YES
49	0.0381	23.6552	7.0022	0.0383	3.0861	13.4142	Lip	YES
50	0.0367	3.2249	2.0097	4.0454	2.7286	4.4868	BSA	YES
51	0.0365	47.5912	1.0886	-0.0317	0.5385	2.8833	Amy	YES
52	-0.0249	5.3064	0.0251	-0.0541	3.0858	5.1605	Fer	YES
53	0.0265	25.0879	1.0192	0.0353	0.5735	7.2697	Lys	YES
54	-0.0217	4.1281	0.1720	-0.0463	5.0178	4.4913	Fer	YES
55	0.0197	18.1657	7.0109	0.0497	7.5318	11.8303	Lip	YES
56	0.0453	47.2604	2.0273	-0.0354	0.6315	3.3308	Amy	YES
57	-0.0195	3.7982	1.2125	4.0348	2.5901	2.6594	BSA	YES
58	-0.0167	14.0147	0.2106	-0.0469	0.1838	12.1914	HSA	YES
59	0.0454	4.0803	1.2043	5.0537	2.4238	3.1062	BSA	YES
60	0.0405	41.4076	1.1746	-0.0591	0.9762	2.8994	Amy	YES

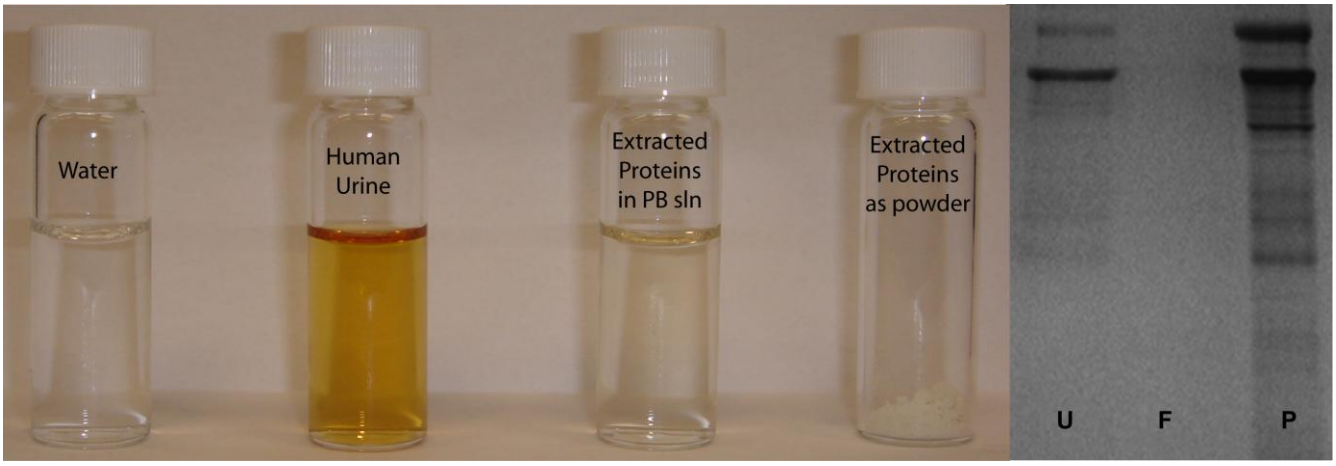

Figure S27. These pictures compare the physical state and color of the concentrated human urine proteins with the original human urine samples (water is used as reference in terms of both turbidity and color). On the gel electrophoresis,[7] no urine proteins are lost during the binding step, as can be seen by examining the binding flowthrough. Line U is 30 µL of input human urine, line F is the binding flowthrough, and line P is 30 µL of the eluted protein.

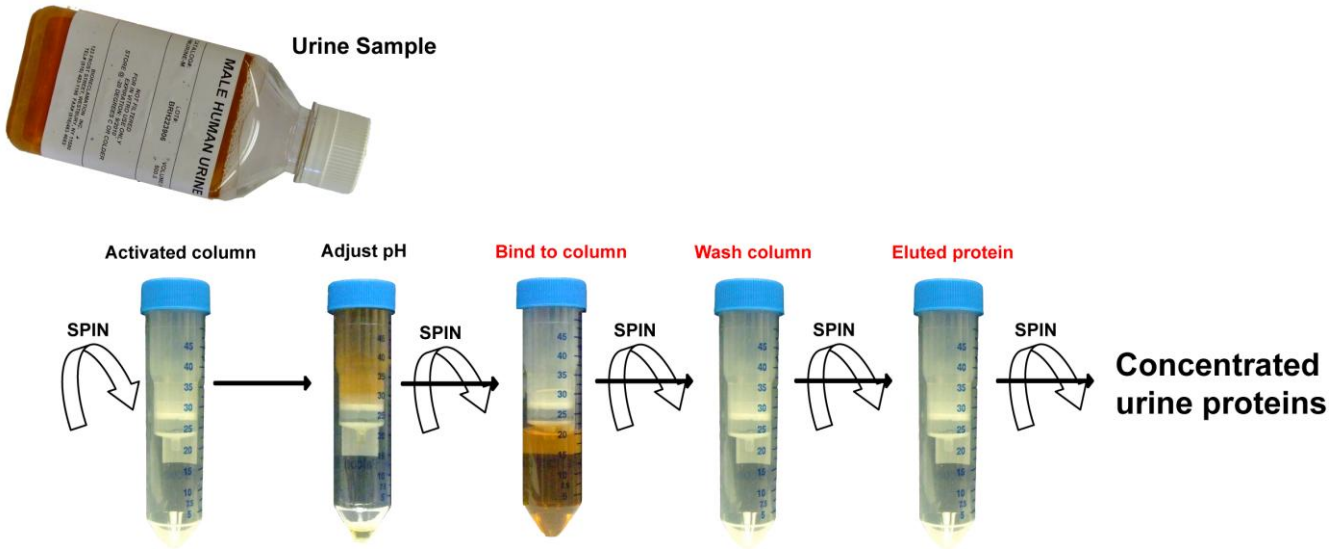

Figure S28. Protein purification. Purification is based on spin column chromatography using Norgen's property resin as an ion exchanger. The resin has poor affinity for monovalent and divalent cations, making it an effective resine removal of salts. Urine proteins are preferentially purified from all other urine components including salts and other wastes.

[7] Proteospin Urine Protein Concentration Kits, Norgen Biotek Corporation.

Table S5. Sources of urine proteins including soluble proteins and protein components of solid phase elements.[8]

Sources of urinary proteins	Comments
Soluble proteins	
• Glomerular filtration of plasma proteins	• Normally present (< 150 mg/day). • Defects in glomerular filter increase high molecular weight protein (e.g. albumin) excretion. • Defects in proximal tubule reabsorption or abnormal production of low molecular weight plasma proteins increase low molecular weight protein (e.g. β2-microglobulin, immunoglobulin light chains retinol-binding protein, and amino acids) excretion.
• Epithelial cell secretion of soluble proteins	• Via exocytosis (e.g. epidermal growth factor) or glycosylphosphatidyl inositol (GPI) anchored protein detachment (e.g. Tamm-Horsfall protein).
Solid phase components	
• Epithelial cells - Whole cell shedding	• Increased cell number compatible with several diseases including acute tubular necrosis (e.g. renal tubule cell shedding) and glomerular diseases (e.g. podocyte shedding).
- Plasma membrane and intracellular component shedding	• Could be due to non-specific, nephrotoxic, or apoptotic processes.
- Exosome secretion	• Normal process, see "Proteomics of Urinary Exosomes".
• Other cells	• In certain diseases, red blood cells, white blood cells, or tumor cells (e.g. bladder cancer and lymphoma) can be present in urine.

Note that epithelial cells include all epithelial cells along urinary tract starting from podocytes to urethral epithelia

[8] Pisitkun, T.; Johnstonen, R.; Knepper, M. A. *Mol. Cell. Proteomics* **2006,** 5, 1760.

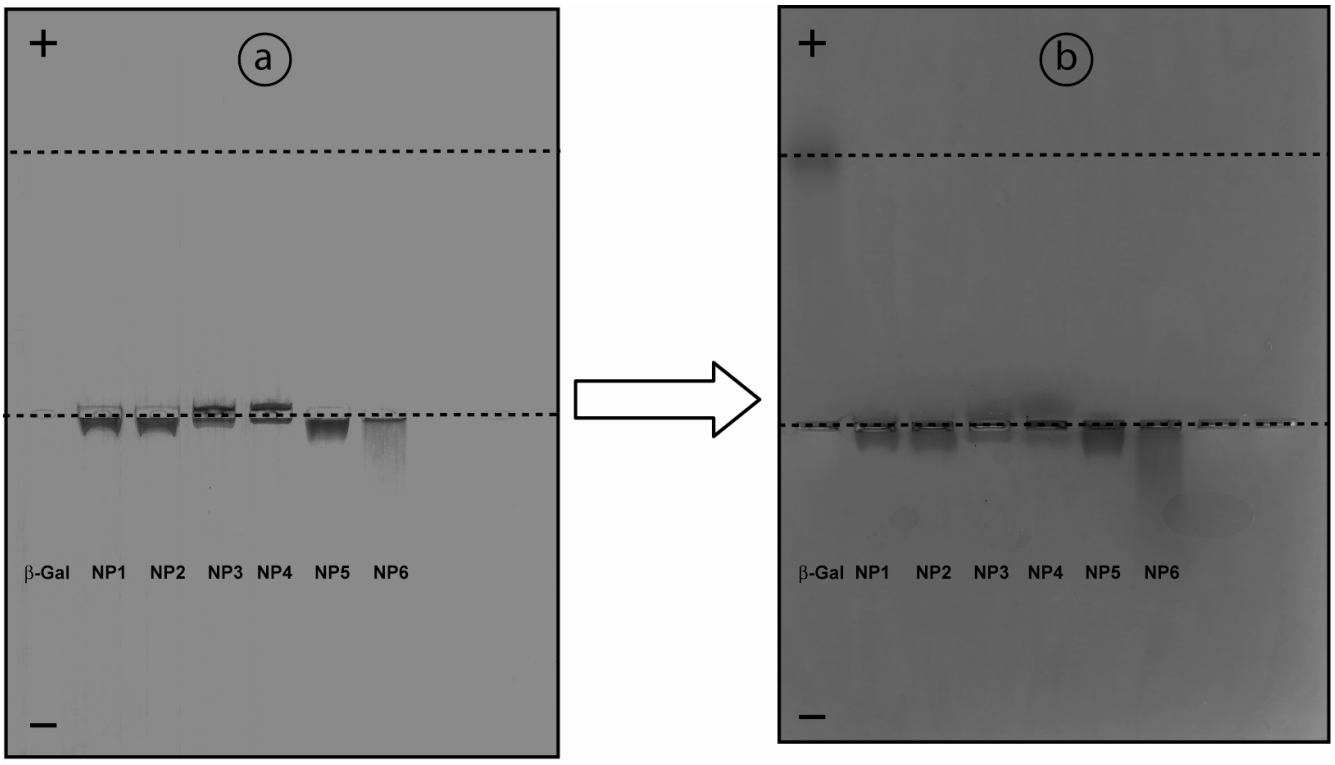

Samples (n =6)	Ligand shell composition *	Core size (nm) §	D_H (nm) †	ζ Potential (mV) ‡	Chemical structure of Ligands £
β-Gal	—	—	18.55 ± 1.71	– 22.67 ± 1.53	Large, tetrameric enzyme, Mw = 465 kDa
NP1	100% L1	2.15 ± 0.28	12.12 ± 0.10	+ 22.30 ± 0.31	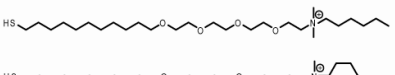
NP2	100% L2	2.09 ± 0.27	10.33 ± 0.15	+ 21.20 ± 0.10	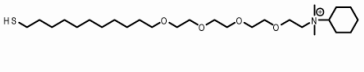
NP3	100% L3	2.12 ± 0.21	12.13 ± 0.07	+ 20.13 ± 0.57	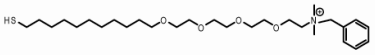
NP4	100% L4	2.14 ± 0.25	12.50 ± 0.11	+ 20.10 ± 0.22	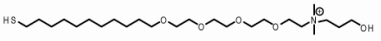
NP5	100% L5	2.10 ± 0.29	13.31 ± 0.08	+ 22.53 ± 0.19	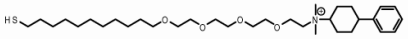
NP6	100% L6	2.11 ± 0.22	17.75 ± 0.03	+ 25.17 ± 0.03	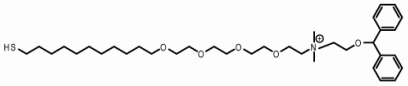

* Calculated from ^{1}H NMR spectra.

§ Determined by TEM images , image J and Origin 7.0 and expressed as average diameter ± standard deviation.

† Hydrodynamic diameter (D_H) measurements are in 5 mM phosphate buffer at pH 7.40.

‡ Zeta potential measurements are in 5 mM phosphate buffer at pH 7.40.

£ Determined from ^{1}H NMR spectra at 400 MHz.

Figure S29. Gel electrophoresis of β-gal and nanoparticles **NP1**-**NP6**: a) before staining and b) after staining. The concentration of enzyme was fixed at 8 μM as well as **NP1**-**NP6** concentrations. The average size of the core metal was determined from a population of 200 nanoparticles by both TEM and image J and expressed in average diameter ± its standard deviation between runnings. Zeta potential were measurements in 5 mM phosphate buffer, pH = 7.4.

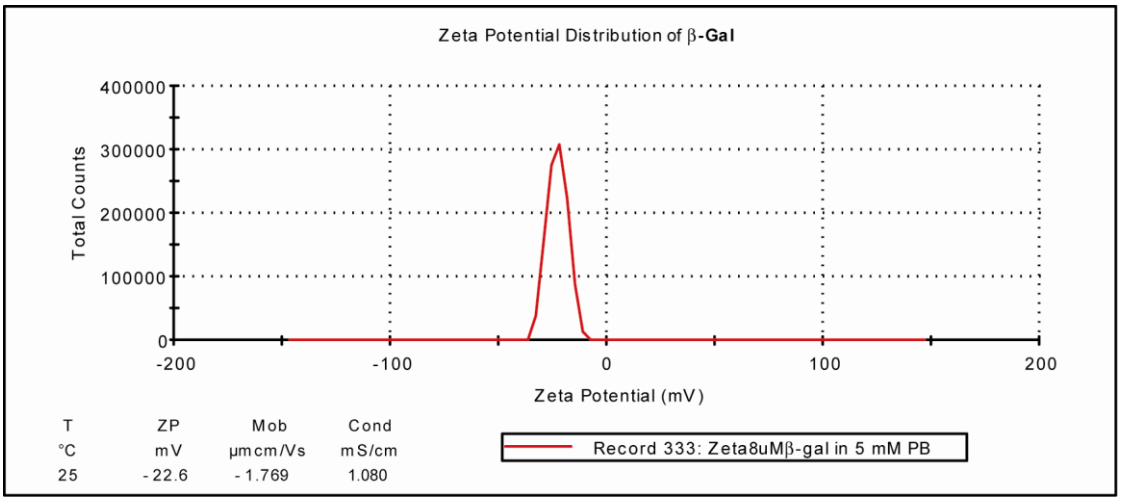

Figure S30. Zeta potential of β-Gal was measured in 5 mM phosphate buffer at pH 7.4. The charge average of β-Gal was -22.67 ± 1.53 mV.

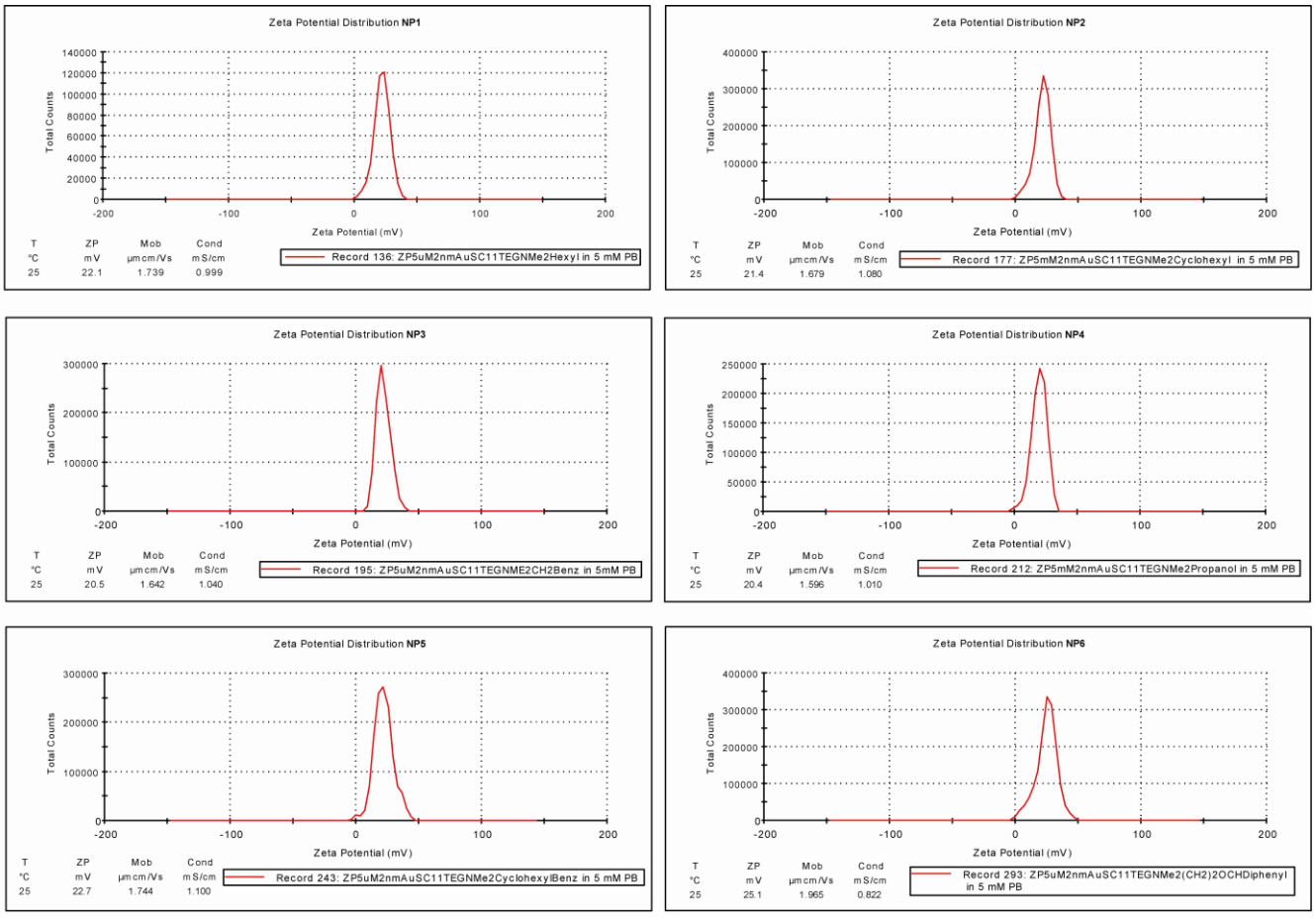

Figure S31. Zeta potential of **NP1-NP6** was measured in 5 mM phosphate buffer at pH 7.4. The overall charges of these cationic AuNPs are on the range of + 20-25 mV.

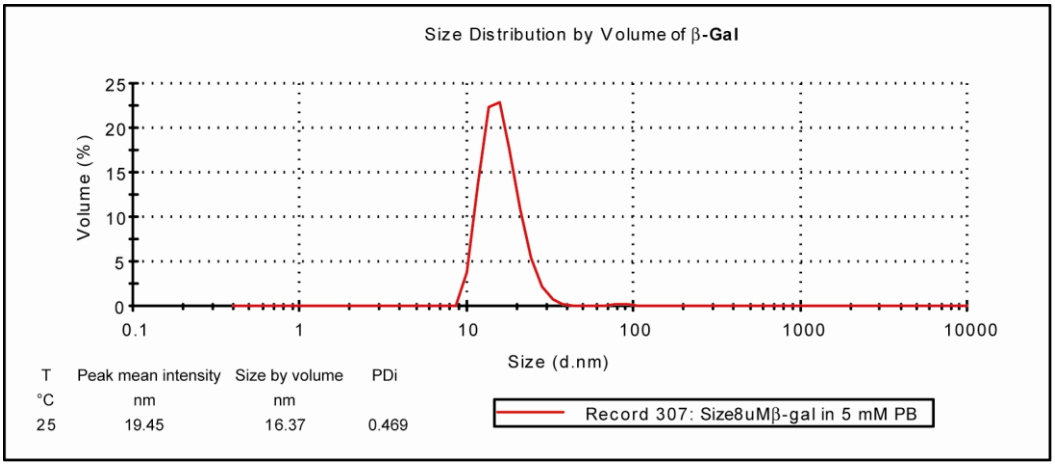

Figure S32. Dynamic light scattering (DLS) of β-Gal was measured in 5 mM phosphate buffer at pH 7.4. The size average of β-Gal was 18.55 ± 1.71 nm.

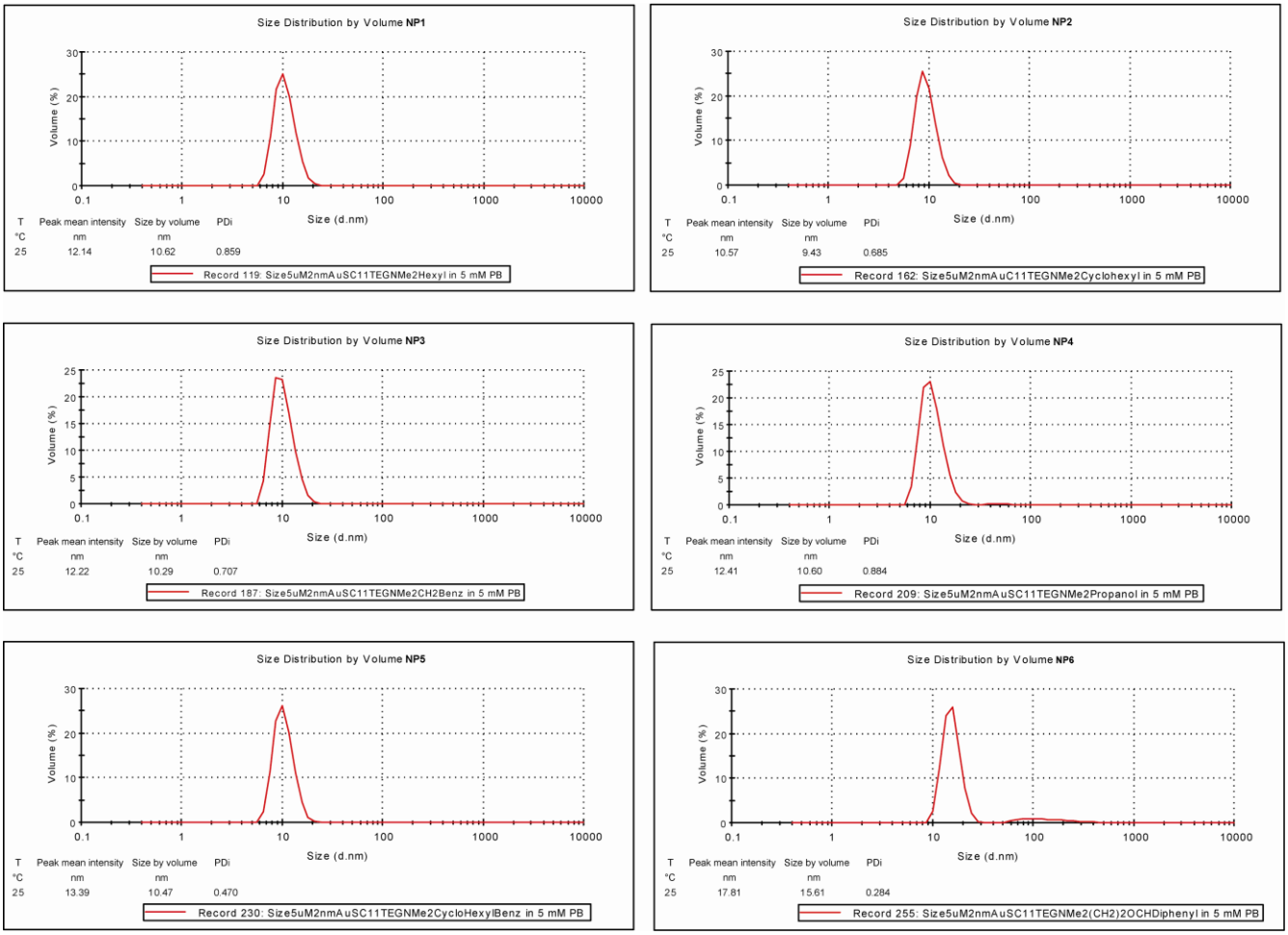

Figure S33. Dynamic light scattering (DLS) of **NP1-NP6** was measured in 5 mM phosphate buffer at pH 7.4. The overall sizes of these cationic AuNPs are on the range of 10.57-17.81 nm.

Table S6. Physical properties of the proteins used as sensing targets in phosphate buffer solution at pH 7.4.

Samples‡ (n = 6)	**D_H^* (nm)**	**ζ Potential (mV)**	**$\varepsilon_{280} = M^{-1} cm^{-1}$**
α-Amylase (α-Am)	7.8±0.4 (0.432)	-8.6±0.9	130000
Bovine serum albumin (BSA)	8.9±0.3 (0.317)	-10.3±0.1.4	46860
Cytochrome *c* (CytC)	4.4±0.5 (0.317)	+6.29±1.5	23200
Ferritin (Fer)	27.3±0.9 (0.251)	-21.7±3.2	950000
Human serum albumin (HSA)	7.6±0.5 (0.707)	-8.8±0.1.8	37800
Lipase (Lip)	4.9±0.8 (0.493)	-12.1±0.7	54350
Lysozyme (Lys)	3.9±0.5 (0.317)	+4.5±0.5	38000
Myoglobin (Myo)	4.6±0.3 (0.668)	-12.5±0.3	13940
Alkaline phosphatase (PhosB)	13.1±0.7 (0.459)	-17.6±1.4	62780

D) retemaid cimanydordyh eht ot tnecajda sisehtnerap ehT :etoN$^*_H$) is the corresponding polydispersity index.

‡ Proteins in *italics* are found in human urine.

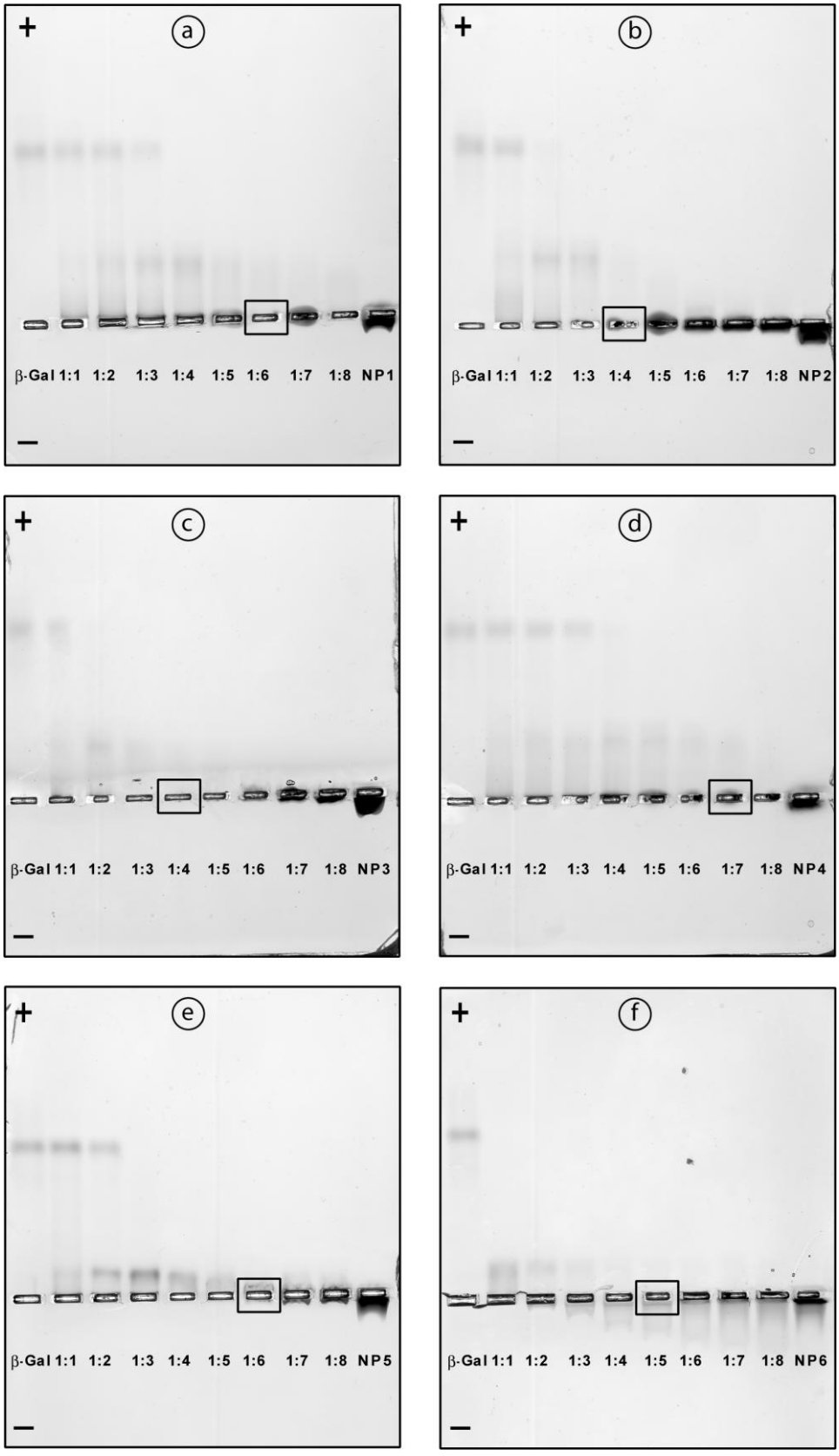

Figure S34. Gel electrophoresis of β-Gal and AuNPs with varying molar ratios (enzyme-AuNP adducts) of a) **NP1**, b) **NP2**, c) **NP3**, d) **NP4**, e) **NP5**, and f) **NP6**. The concentration of the enzyme was 2 μM.

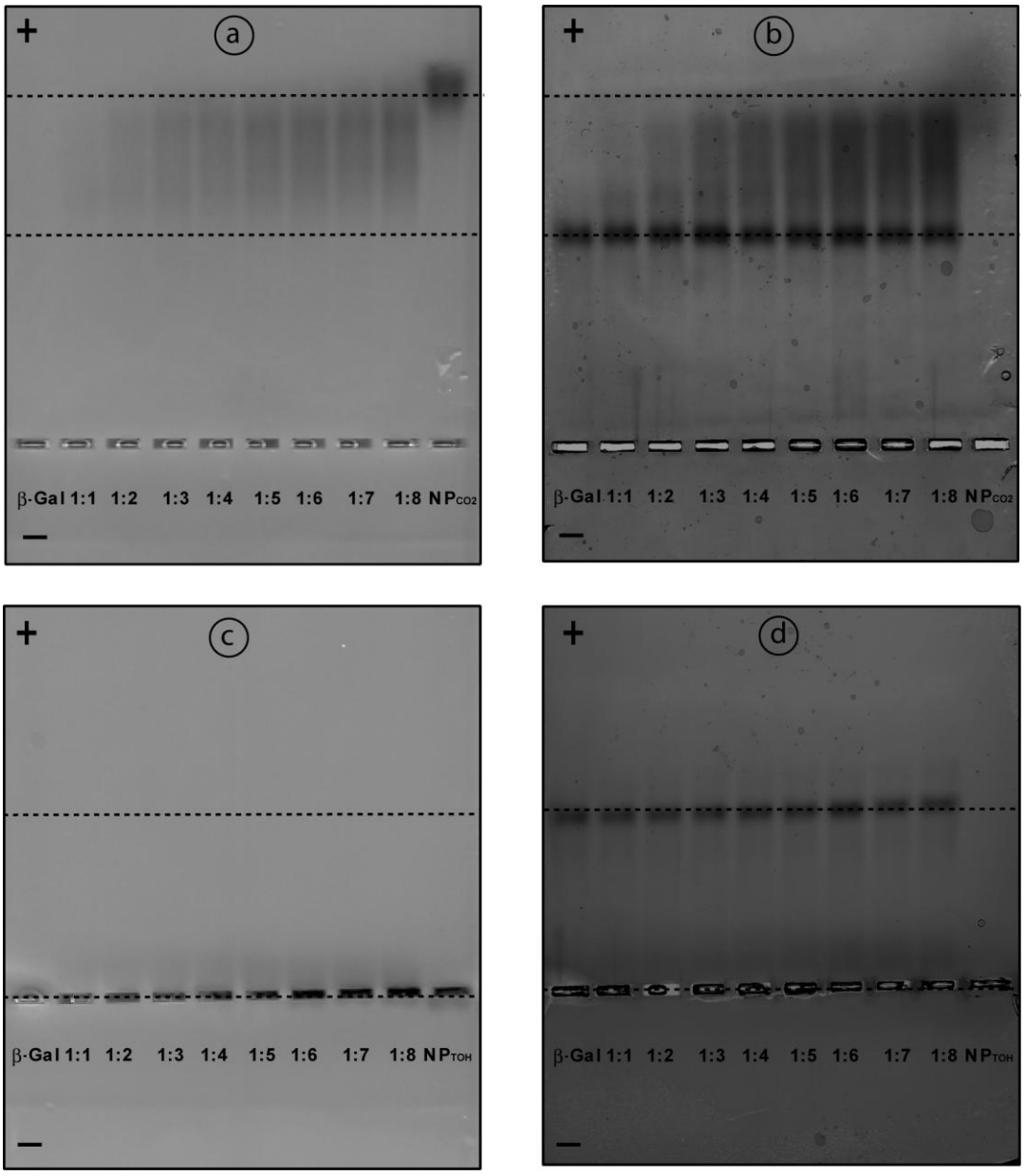

Figure S35. As control experiment, gel electrophoresis of β-Gal and both negative charge $\mathbf{NP_{CO2}}$ (26-mercapto-3,6,9,12,15-pentaoxahexacosan-1-oate capping the metal core)[9] and neutral charge $\mathbf{NP_{OH}}$ **(**23-mercapto-3,6,9,12-tetraoxatricosan-1-ol capping the metal core) with varying molar ratios (enzyme: NP) of a) before staining $\mathbf{NP_{CO2}}$, b) after staining $\mathbf{NP_{CO2}}$, c) before staining $\mathbf{NP_{OH}}$, d) after staining $\mathbf{NP_{OH}}$. The concentration of the enzyme was 2 μM. As it can be seen on the gels b) and d) anionic AuNPs and neutral AuNPs do not interact strongly with the enzyme, β-Gal**.**

[9] Hong, R.; Fischer, N. O.; Verma, A.; Goodman, C. M.; Emrick, T.; Rotello, V. R. *J. Am. Chem. Soc.*, **2004**, *126*, 739

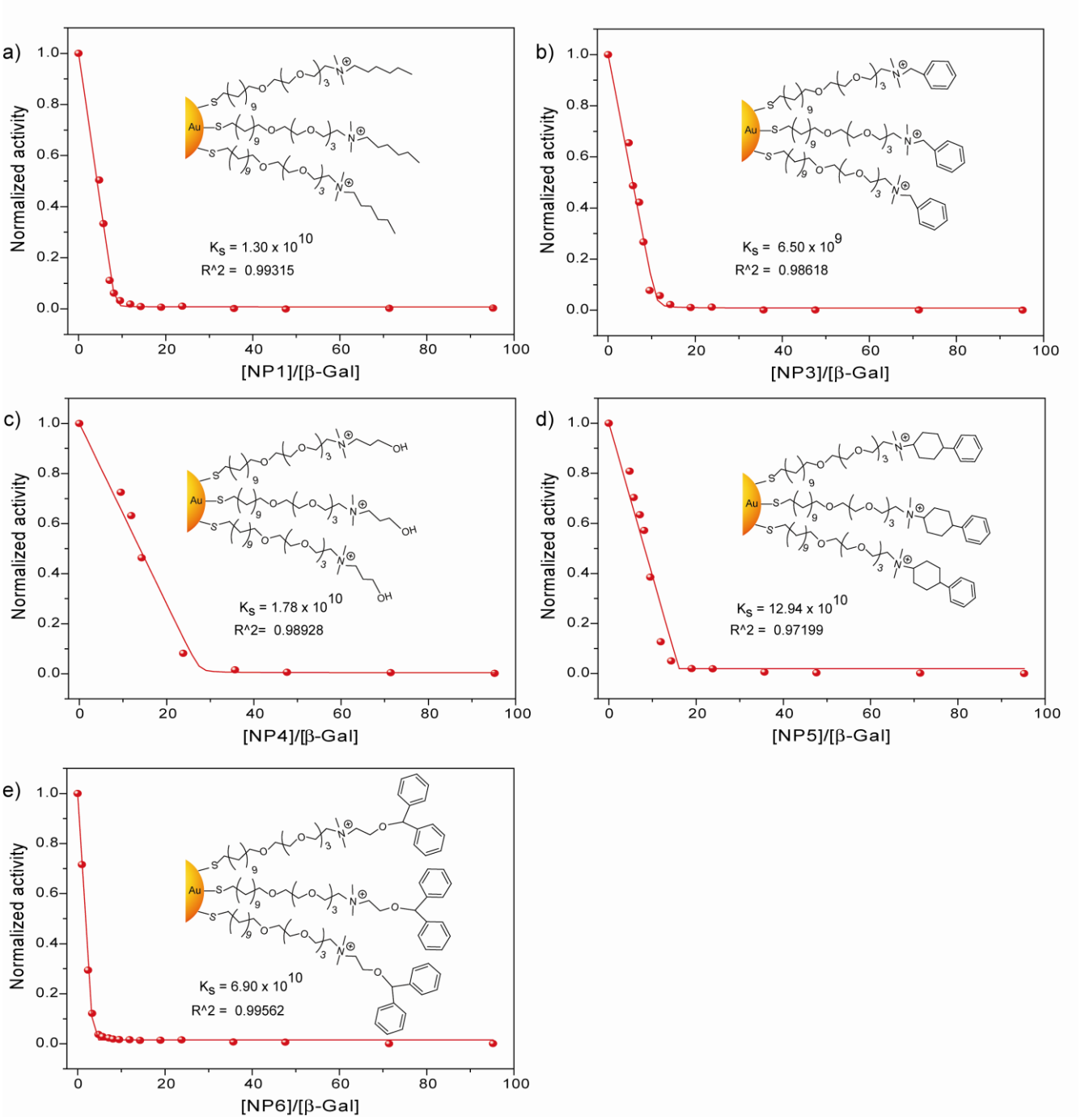

Figure S36. Fluorescence titration curves for the complexation of β-Gal (0.5 nM) with cationic gold nanoparticles (**NP1**-**NP6**). The inhibition study was measured following the addition of cationic nanoparticles (0-100 nM) with an excitation wavelength of 455 nm.

Thermodynamic parameters for the enzyme-nanoparticle conjugates

Both the binding constant (Ks) and the binding ratio (n) between β-Gal and AuNPs could be quantified using the activity titration curves through nonlinear least-squares curve fitting analysis combined with gel electrophoresis. The experimental ratios of nanoparticles to β-Gal needed to yield ~1% enzyme activity ranged from 4.0 for **NP2**-**NP3** to 7.0 for **NP1** (see Table S7 and Figure S36). The inhibition of β-Gal activity strongly depends on the chemical structural changes of the peripheral ligands on the AuNPs, as shown in Table S7. Complex stabilities vary within approximately one order of magnitude ($\Delta\Delta G \approx 9$ KJ mol^{-1}), and the binding stoichiometry (n) between each AuNP and the enzyme vary from 4 to 7, since they possess different affinity. These observations indicate that the subtle structural changes of the nanoparticles end groups significantly affect the affinity for the enzyme. Under these conditions, it is estimated that >80% of **NP1**-**NP6** is bound to the β-Gal, based on the binding constant listed on Table S7, allowing fluorescence enhancement through both subsequent displacement enzymatic reaction.

Table S7. Binding constants (K_S) and binding stoichiometries (n) between β-Gal and several cationic nanoparticles (**NP1**–**NP6**) in desalted urine as determined from both activity assays and gel.

Nanoparticles	K_S (10^{10} M^{-1})	-ΔG (kJ mol^{-1})	*n*
NP1	1.30	57.3	6
NP2	0.31	53.8	4
NP3	0.65	55.6	4
NP4	1.78	58.1	7
NP5	12.94	63.0	6
NP6	6.90	61.4	5

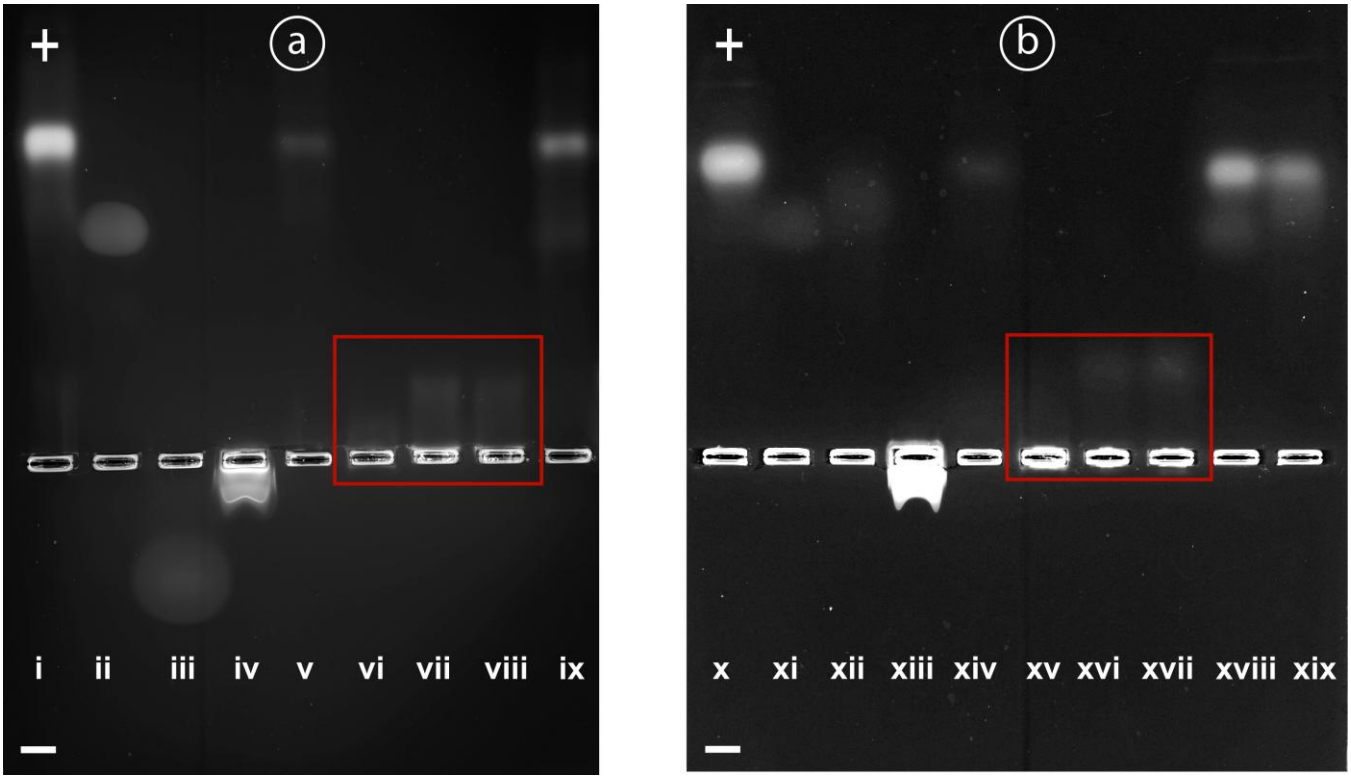

Figure S37. Gel electrophoresis confirms the hypothesis that the displacement assays of the enzyme by proteins take place. **Agarose gel electrophoresis a)** shows the displacement assay of β-Gal by two proteins HSA (-) and lysozyme (+): i) 8 μM β-Gal, ii) 8 μM HSA (notes that the broad peak is probably due to high concentration of the protein), iii) Lysozyme (notes that the broad peak is probably due to high concentration of the protein), iv) 8 μM **NP2**, v) 2 μM of β-Gal and 8 μM $\mathbf{NPT_{OH}}$, vi) 1:4 molar ratio (enzyme : **NP2**), vii) 1:4 molar ratio (β-Gal : **NP2**) and 1 μM HSA, viii) 1:4 molar ratio (enzyme : **NP2**) and 1 μM lysozyme and ix) 2 μM β-Gal and 1 μM HSA confirming the no interaction between these two proteins. **Agarose gel electrophoresis b)** shows the displacement assay of β-Gal by two proteins BSA (-) and Ferritin (-): x) 8 μM β-Gal, xi) 8 μM BSA (notes that the broad peak is probably due to high concentration of the protein), xii) Ferritin (notes that the broad peak is probably due to high concentration of the protein), xiii) 8 μM **NP2**, xiv) 2 μM of β-Gal and 8 μM $\mathbf{NPT_{OH}}$, xv) 1:4 molar ratio (β-Gal : **NP2**), xvi) 1:4 molar ratio (enzyme : **NP2**) and 1 μM BSA, xvii) 1:4 molar ratio (enzyme : **NP2**) and 1 μM Ferritin, xviii) 2 μM β-Gal and 1 μM BSA confirming that there is no interaction between these two proteins and xix) 2 μM β-Gal and 1 μM Ferritin confirming that there is no interaction between them.

Table S8. Final and initial kinetics ratio of the fluorescence response patterns of β-Gal and six AuNPs (**NP1**-**NP6**) adducts against various target proteins ± standard deviation (SD). Each value represents an average of six parallel measurements.

Proteins	($V_{max}/V_{o,max}$)											
	NP1	*SD*	*NP2*	*SD*	*NP3*	*SD*	*NP4*	*SD*	*NP5*	*SD*	*NP6*	*SD*
α-Amy	1.162744	0.089064	3.828086	0.335818	2.401873	0.169194	0.482782	0.089669	1.045633	0.017870	1.581139	0.088925
BSA	0.566856	0.045598	1.357927	0.215107	1.456985	0.202390	0.870069	0.056741	1.165084	0.078856	1.923542	0.538564
CytC	1.020838	0.008033	1.349411	0.095001	1.657639	0.158399	1.027977	0.021659	1.171242	0.046114	1.486211	0.199757
Fer	0.998399	0.002915	1.731210	0.209064	1.044367	0.013751	1.009791	0.047099	1.570519	0.305616	1.825326	0.250235
HSA	1.022090	0.093190	0.578550	0.061970	0.593520	0.082680	1.053750	0.020060	0.198600	0.078690	1.067530	0.030660
Lip	1.142678	0.111317	1.119827	0.032988	2.167052	0.265922	0.462804	0.448489	1.368664	0.163287	1.414100	0.097572
Lys	1.214415	0.071499	2.421471	0.231323	1.189766	0.081647	1.006598	0.004832	1.015704	0.008186	2.421105	0.244526
Myo	1.212988	0.055828	1.310051	0.153280	1.320058	0.194570	1.413432	0.059226	1.109101	0.036296	2.249909	0.278100
PhosB	1.017318	0.008850	1.480974	0.207608	2.102657	0.339915	1.010170	0.009593	1.048541	0.033976	2.465599	0.190674

Table S9. Training matrix of activity response patterns generated from β-Gal/AuNP sensor array (**NP1**–**NP6**) and the fluorogenic substrate (4-Methylumbelliferyl-beta-D-galactopyranoside) against various proteins (concentration = 1 nM).†

Protein	**NP1**	**NP2**	**NP3**	**NP4**	**NP5**	**NP6**
α-Amy	0.160975	3.393432	1.251925	-0.499563	0.072658	0.786185
α-Amy	0.119801	2.838373	1.658166	-0.359135	0.065237	0.664113
α-Amy	0.360905	3.525645	1.576092	-0.578533	0.042495	0.617349
α-Amy	0.123519	3.427957	1.378307	-0.575258	0.037157	0.557427
α-Amy	0.146484	3.781986	1.276771	-0.552547	0.021673	0.549194
α-Amy	0.119801	2.805677	1.594953	-0.614698	0.047126	0.540163
BSA	-0.524773	0.855423	0.368644	-0.042752	0.112765	1.699626
BSA	-0.407967	0.518049	0.358356	-0.212016	0.144267	0.408964
BSA	-0.435635	0.122587	0.872029	-0.177976	0.304944	1.674564
BSA	-0.425384	0.344485	0.444321	-0.122473	0.117598	0.454712
BSA	-0.440822	0.281023	0.286352	-0.129752	0.245323	0.838603
BSA	-0.510731	0.380946	0.518147	-0.113815	0.110997	0.826483
CytC	0.035445	0.235972	0.477981	0.018681	0.149347	0.689965
CytC	0.016592	0.487015	0.726525	0.010589	0.152206	0.731896
CytC	0.018037	0.474577	0.569288	0.029653	0.175445	0.291318
CytC	0.025684	0.317109	0.925419	0.040126	0.184414	0.389811
CytC	0.011405	0.520908	0.601658	0.067659	0.141485	0.705795
CytC	0.024912	0.407391	0.797416	0.005288	0.271643	0.298903
Fer	0.003009	0.706992	0.048231	0.108201	0.175369	0.911452
Fer	-0.004823	0.685545	0.037454	-0.014575	0.527787	1.088146
Fer	-0.002341	1.132817	0.033757	-0.010029	0.560338	1.103283
Fer	-0.000267	0.886735	0.067819	-0.003723	1.111381	1.023901
Fer	-0.005135	1.139926	0.034846	-0.006647	0.778952	0.737603
Fer	-0.000593	0.560372	0.054377	-0.013032	0.426158	0.410803
HSA	0.156082	-0.007475	-0.049664	0.065918	-0.173453	0.044086
HSA	0.008484	-0.068359	-0.084735	0.041808	-0.152816	0.126597
HSA	0.017289	-0.078791	0.045644	0.054551	-0.074029	0.069858
HSA	-0.050856	-1.088342	-0.127892	0.075639	-1.088317	0.034675
HSA	0.114875	-1.690797	-0.146809	0.071153	-1.556754	0.071189
HSA	-0.105869	-0.012866	-2.169627	0.021359	-1.983362	0.085226
Lip	0.146105	0.110819	1.179293	-0.316738	0.272846	0.578538
Lip	0.071871	0.119053	1.110435	-0.341516	0.325371	0.453623

Lip	0.287884	0.188278	1.532652	-0.442879	0.551288	0.268081
Lip	0.272863	0.189773	1.480295	-0.468783	0.223874	0.505244
Lip	0.145567	0.110815	1.199872	-0.258125	0.294458	0.427209
Lip	-0.019982	0.119053	0.770309	-1.474511	0.645517	0.414082
Lys	0.157841	1.338209	0.276587	0.003676	0.026419	1.161619
Lys	0.345268	1.835289	0.322254	0.015918	0.006708	1.443934
Lys	0.152547	1.650511	0.153046	0.006084	0.018897	1.793173
Lys	0.187049	1.324925	0.183459	0.006877	0.006816	1.822576
Lys	0.276511	1.837733	0.100717	0.001406	0.014839	1.538729
Lys	0.239768	1.951802	0.146523	0.006601	0.024864	1.323167
Myo	0.278681	0.571847	0.506194	0.510292	0.155658	1.569218
Myo	0.278686	0.326684	0.299995	0.391116	0.091697	0.981664
Myo	0.147753	0.502119	0.493531	0.378591	0.167591	1.254026
Myo	0.213595	0.412139	0.505887	0.457545	0.090003	1.571516
Myo	0.163881	0.287045	0.137232	0.455627	0.097038	0.993984
Myo	0.267342	0.067942	0.051702	0.348509	0.082618	1.618565
PhosB	0.005053	0.365723	0.980838	0.005815	0.037872	1.771964
PhosB	0.016418	0.589436	1.440413	0.023637	0.044395	1.485478
PhosB	0.017679	0.39391	1.654379	-0.000182	0.112109	1.661552
PhosB	0.032841	0.576594	0.756166	0.001841	0.025471	1.323127
PhosB	0.019104	0.971739	1.202948	0.014152	0.029686	1.774132
PhosB	0.018667	0.465411	0.836812	0.017257	0.05506	1.351331

† β-Gal: β-galactosidase, ε (280 nm) = 1128600 M^{-1} cm^{-1}; BSA: bovine serum albumin, ε (280 nm) = 46860 M^{-1} cm^{-1}; α-Amy: α-amylase, ε (280 nm) = 130000 M^{-1} cm^{-1}; PhosB: alkaline phosphatase, ε (280 nm) = 62780 M^{-1} cm^{-1}; Myo: myoglobin, ε (280 nm) = 13940 M^{-1} cm^{-1}; HSA: human serum albumin, ε (280 nm) = 37800 M^{-1} cm^{-1}; CytC: cytochrome *c*, ε (280 nm) = 23200 M^{-1} cm^{-1}; Lip: lipase: ε (280 nm) = 54350 M^{-1} cm^{-1}; Fer: ferritin: ε (280 nm) = 950000 M^{-1} cm^{-1}; Lys: lysozyme: ε (280 nm) = 38000 M^{-1} cm^{-1}.

Table S10. Accuracy of LDA classification of protein analytes (Conc. = 1 nM) from the complexes of the enzyme (β-Gal) with individual cationic nanoparticles as sensors. The values are taken from the Jackknifed classification matrix based on LDA analysis of the raw data (6 replicates) listed in Table S2.

Protein	**NP1-** (β-Gal)	**NP2-** (β-Gal)	**NP3-** (β-Gal)	**NP4-** (β-Gal)	**NP5-** (β-Gal)	**NP6-** (β-Gal)
α-Amy	0%	100%	67%	17%	50%	33%
BSA	100%	0%	33%	83%	17%	0%
CytC	0%	17%	50%	33%	33%	0%
Fer	100%	50%	100%	0%	67%	17%
HSA	0%	33%	17%	67%	50%	100%
Lip	33%	100%	17%	0%	33%	50%
Lys	0%	100%	50%	83%	100%	17%
Myo	0%	33%	17%	100%	67%	17%
PhosB	67%	33%	17%	0%	17%	50%
Total	33%	52%	41%	43%	48%	31%

Table S11. Identification of 60 unknowns protein samples with LDA using β-Gal/AuNP sensor array.

Entry	Fluorescence response pattern						Identification	Accuracy
	NP1- (β-Gal)	**NP2-** (β-Gal)	**NP3-** (β-Gal)	**NP4-** (β-Gal)	**NP5-** (β-Gal)	**NP6-** (β-Gal)	Proteins	YES/NO
1	0.014053	0.725769	1.387652	0.005863	0.038725	1.576353	PhosB	YES
2	0.258481	0.490884	0.268747	0.458737	0.092778	1.437691	Myo	YES
3	0.011883	0.521188	0.616283	0.059383	0.159981	0.757299	CytC	YES
4	0.014982	0.519524	0.837249	0.032874	0.198373	0.629875	CytC	YES

5	0.018655	0.578776	0.987652	0.002845	0.024236	1.654218	PhosB	YES
6	0.123629	3.417971	1.373303	-0.574268	0.031153	0.553475	α-Amy	YES
7	0.015273	0.435886	0.858873	0.032992	0.198745	0.498731	CytC	YES
8	0.153256	0.188375	0.476772	0.510535	0.126633	1.352787	Myo	YES
9	0.129887	-0.098539	-0.079845	0.057954	-0.398851	0.096358	HSA	YES
10	0.260995	3.124645	1.560927	-0.478231	0.062795	0.617343	α-Amy	YES
11	0.024187	0.693764	1.469739	0.017652	0.044163	1.678362	PhosB	YES
12	-0.498358	0.273985	0.862731	-0.182616	0.239642	0.947846	BSA	YES
13	0.136414	3.683982	1.275778	-0.392842	0.031974	0.657194	α-Amy	YES
14	0.028965	0.649875	0.997631	0.016238	0.054543	1.423162	PhosB	YES
15	-0.454561	0.231843	0.792837	-0.173653	0.291861	1.629482	BSA	YES
16	0.302952	1.629439	0.183849	0.006896	0.018905	1.239049	Lys	YES
17	0.150965	2.934324	1.351625	-0.593519	0.042638	0.563719	α-Amy	YES
18	0.017873	0.939473	1.202948	0.014322	0.032645	1.736251	PhosB	YES
19	0.184932	0.209837	0.197235	0.456526	0.153874	0.152663	Myo	YES
20	0.217752	0.146651	1.135246	-0.419791	0.257746	0.351247	Lip	NO
21	0.187493	2.965968	1.275778	-0.534757	0.057723	0.627548	α-Amy	YES
22	-0.503725	0.489471	0.629473	-0.122792	0.147662	0.793848	BSA	YES
23	0.009714	-0.059456	-0.048769	0.039845	-1.098469	0.118985	HSA	YES
24	0.293129	1.498453	0.307858	0.003982	0.013851	1.497034	Lys	YES
25	-0.013265	0.102732	0.936304	-1.498739	0.615528	0.317413	Lip	YES
26	0.023876	0.362539	0.918031	0.042857	0.298437	0.393148	CytC	YES
27	-0.002182	1.112349	0.039762	-0.015416	0.929874	0.577653	Fer	YES
28	-0.421627	0.497436	0.463785	-0.114537	0.182949	1.459478	BSA	YES
29	0.028768	0.470821	0.758837	0.007925	0.239754	0.621475	CytC	YES
30	0.199835	1.593782	0.153952	0.005039	0.007942	1.374757	Lys	YES
31	0.258763	0.175245	1.562535	-0.865528	0.638771	0.456171	Lip	YES
32	-0.453511	0.467336	0.518487	-0.172652	0.218672	0.635572	BSA	YES
33	0.128634	0.188264	1.329782	-0.562564	0.296625	0.498782	Lip	YES
34	-0.050942	-0.907456	-0.876578	0.079871	-1.548758	0.087461	HSA	YES
35	0.273827	1.358371	0.296496	0.014713	0.006183	1.320896	Lys	YES
36	-0.004126	1.076529	0.047659	-0.002942	0.987631	0.678657	Fer	YES
37	-0.504781	0.187457	0.638245	-0.115578	0.142746	1.538495	BSA	YES
38	-0.000318	0.981453	0.070842	-0.001639	0.887382	1.017295	Fer	NO
39	0.003155	0.936953	0.052171	-0.010561	0.176537	1.081474	Fer	YES
40	0.225627	3.383681	1.476634	-0.413654	0.042795	0.557614	α-Amy	YES
41	-0.000341	0.983735	0.042988	-0.018775	0.987663	0.654926	Fer	YES
42	-0.479739	0.180497	0.519372	-0.139839	0.169624	0.408965	BSA	YES
43	0.193275	0.502132	0.507256	0.377671	0.156627	1.275536	Myo	YES
44	-0.003987	0.749757	0.042145	-0.014287	0.538756	0.827541	Fer	NO
45	0.175627	0.168979	1.261547	-0.652531	0.342883	0.463789	Lip	NO
46	0.129301	2.893649	1.571664	-0.456148	0.055136	0.636467	α-Amy	YES
47	0.035294	0.479481	1.531231	-0.001693	0.112352	1.466216	PhosB	NO
48	0.223183	0.374849	0.372634	0.451267	0.142731	0.996628	Myo	YES
49	0.224348	0.394871	0.351719	0.376235	0.112835	1.618565	Myo	YES
50	0.179835	1.529733	0.164895	0.015324	0.008231	1.524564	Lys	YES
51	0.097657	-0.087756	-1.287873	0.048752	-1.246568	0.107367	HSA	YES
52	-0.414592	0.598458	0.628468	-0.198481	0.212453	0.683825	BSA	YES
53	0.013626	0.493882	0.721265	0.019386	0.247387	0.987563	CytC	YES
54	0.106479	-0.678467	-1.974631	0.057439	-0.74631	0.097364	HSA	YES
55	0.217583	1.712908	0.243952	0.009737	0.001754	1.684731	Lys	YES
56	0.259853	1.824312	0.168956	0.006139	0.021745	1.302892	Lys	YES
57	-0.431676	0.529435	0.618468	-0.151652	0.161652	1.605218	BSA	YES
58	0.011834	-0.087646	-1.098136	0.069973	-0.90853	0.084627	HSA	NO
59	0.115538	0.146251	1.987377	-0.252165	0.572532	0.476556	Lip	YES
60	0.118801	2.825617	1.514973	-0.615836	0.049129	0.582761	α-Amy	YES